UNIVERSIDADE FEDERAL DE SANTA CATARINA
DEPARTAMENTO DE ENGENHARIA MECÂNICA

Mateus Viana de Oliveira e Costa

FORCE CAPABILITY OF PLANAR CABLE-DRIVEN ROBOTS

Florianópolis

2018

Mateus Viana de Oliveira e Costa

FORCE CAPABILITY OF PLANAR CABLE-DRIVEN ROBOTS

Dissertação submetida ao Programa de Pós-Graduação em Engenharia Mecânica para a obtenção do Grau de Mestre em Engenharia Mecânica.
Orientador: Daniel Martins, Dr. Eng.
Coorientador: Henrique Simas, Dr. Eng.

Florianópolis

2018

Ficha de identificação da obra elaborada pelo autor,
através do Programa de Geração Automática da Biblioteca Universitária da UFSC.

Costa, Mateus Viana de Oliveira e
Force capability of planar cable-driven robots / Mateus Viana de Oliveira e Costa ; orientador, Daniel Martins, coorientador, Henrique Simas, 2018.
135 p.

Dissertação (mestrado) - Universidade Federal de Santa Catarina, Centro Tecnológico, Programa de Pós Graduação em Engenharia Mecânica, Florianópolis, 2018.

Inclui referências.

1. Engenharia Mecânica. 2. Robótica. 3. Robôs Paralelos. 4. Robôs por cabos. 5. Capacidade de Força. I. Martins, Daniel. II. Simas, Henrique. III. Universidade Federal de Santa Catarina. Programa de Pós-Graduação em Engenharia Mecânica. IV. Título.

Mateus Viana de Oliveira e Costa

FORCE CAPABILITY OF PLANAR CABLE-DRIVEN ROBOTS

Esta Dissertação foi julgada aprovada para a obtenção do Título de "Mestre em Engenharia Mecânica", e aprovada em sua forma final pelo Programa de Pós-Graduação em Engenharia Mecânica.

Florianópolis, 8 de Junho 2018.

Jonny Carlos da Silva, Dr. Eng.
Coordenador

Daniel Martins, Dr. Eng.
Orientador

Henrique Simas, Dr. Eng.
Coorientador

Banca Examinadora:

Daniel Martins, Dr. Eng.
Presidente

Antônio Otaviano Dourado, Dr. Eng.

Eduardo Alberto Fancello, Dr. Eng.

Rodrigo de Souza Vieira, Dr. Eng.

For the ones who really matters Willia, Joselito, João e Bianca.

AGRADECIMENTOS

Às minhas fontes de inspiração e de amor incondicional, Willia, Joselito e João, por serem minha maior alegria e orgulho. À minha companheira Bianca, por ser sempre tão atenciosa.

Ao sistema federal de ensino, principalmente ao CEFET-MG e à UFSC, por serem partes prepoderantes da minha formação acadêmica e pessoal.

Ao meu orientador, Daniel Martins, por suas observações geniais, por ter acreditado no meu potencial e por ser um exemplo de sucesso e dedicação, além do coração do Laboratório de Robótica. Ao meu coorientador Henrique Simas e ao Leonardo Mejia pelo conhecimento transmitido e ajuda fornecida.

Aos meus mentores informais, Júlio, Thaís e Estevan, por suas orientações sempre acertivas e por estarem sempre disponíveis para ajudar. À minha parceira acadêmica, Marina, aos meus grandes amigos Vinicius Noal, Paulo, Marcel, Vinicius Giacomazzi, Rodrigo, Elias, Vângelo e Fabíola e aos colegas de laboratório Lucas, Luan, André e Camilo. Muito obrigado pelos dois incríveis anos que tivemos.

Aos irmãos que a vida me deu, no CEFET, Gabriel, Leonardo e Guilherme, e da Córeia, De Hong, Lucas e Tiago. Obrigado por estarem sempre ao meu lado.

Ao Programa de Pós-Graduação em Engenharia Mecânica da UFSC, pela oportunidade e apoio indispensável, e ao CNPq e a CAPES pelo apoio financeiro.

Be water, my friend.

Bruce Lee

RESUMO

O desenvolvimento da robótica permitiu que diversas atividades insalubres antes realizadas pelos seres humanos pudessem ser completamente realizadas por manipuladores mecânicos. Com isso, a economia mundial vem se reorganizando e os seres humanos podem concentrar-se em atividades intelectuais. Neste caso, para que esse efeito se amplifique, é necessário que existam dispositivos robóticos capazes de realizar os mais diferentes tipos de atividades e que se adequem às mais diferentes caractéristicas econômicas. Robôs paralelos atuados por cabos, tema central desse trabalho, apresentam-se como um dos dispositivos mais promissores para compor essa nova ordem mundial graças a diversas características. Entre elas, destacam-se o elevado espaço de trabalho, o baixo custo de produção e o rápido enrolamento dos cabos permitindo características dinâmicas únicas. Outro aspecto significativo desse tipo de equipamento é que a flexibilidade dos cabos os tornam mais indicados para interações com seres humanos. Porém, mesmo com todas essas qualidades, diversos aspectos sobre esses dispositivos ainda estão em aberto na academia. Entre eles destaca-se a motivação desse trabalho, que é a capacidade de força desses dispositivos e, a partir dessa informação, a definição de mapas de capacidade de força e do espaço de trabalho wrench-feasible. Para tanto, o primeiro aspecto dessa pesquisa foi definir o modelo matemático que fosse capaz de traduzir todas a estática desse dispositivo. Neste caso, o aspecto de maior complexidade, foi a constante alteração do número de cabos atuados dos dispositivos. Com isso, para que o modelo matemático do robô fosse verossimil, se fez necessário tratá-lo como um dispositivo reconfigurável além de estabelecer leis que representassem tal recofigurabilidade. Concluída a definição dos modelos planares possíveis se fez necessário a definição de métodos capazes de estabelecer a capacidade de força desses manipuladores. Para tanto, o método de Davies foi associado ao método de fator de escala e a otimização com restrições. Um sistema de transição inteligente varia o método de solução de acordo com o modelo atuado do dispositivo. Finalmente, o método proposto por esse trabalho foi definido e consolidado em um algoritmo. Os principais passos do método são a definição dos modelos matemáticos possíveis do robô, o estabelecimento e iteração entre todas as ações à serem aplicadas no efetuador e a solução da capacidade de força para cada um dos passos da iteração utilizando o modelo matemático apropriado. Concluídas essas etapas, um mapa de capacidade de força é definido. Além da definição do método, foram obtidos mapas de capacidade de força para robôs por cabos planares com 2, 3 e 4 cabos além de espaço de trabal-

hos wrench-feasible para configurações com 2 e 3 cabos. Taís informações permitem uma avaliação precisa sobre a capacidade desses dispositivos de realizarem tarefas e seguirem trajetórias que envolvam força. Por último, foi realizada uma comparação entre os resultados obtidos nesse trabalho e algumas pesquisas da literatura. Por fim, o método proposto apresentou-se como mais eficiente, quando comparado com métodos sem a transição inteligente, além de garantir, através do conceito de restrição exata, a pose da plataforma móvel do dispositivo.
Palavras-chave: Robôs por Cabos. Capacidade de Força. Espaço de Trabalho. Estática. Método de Davies.

RESUMO EXPANDIDO

Introdução

Esse projeto de pesquisa propõe a definição da capacidade de força de robôs paralelos planares atuados por cabos. Esse parâmetro de performance é definido como a máxima força ou torque que um manipulador é capaz de aplicar no ambiente ou é capaz de suportar em situações estáticas ou quasi-estáticas. Algumas aplicações da avaliação da capacidade de força são o projeto ótimo de robôs e a definição de características de robôs já construídos como o espaço de trabalho de força e os mapas de capacidade de força. Manipuladores paralelos são mecanismos de cadeia fechada compostos por um efetuador com n graus de liberdade e uma base fixa, conectados através de pelo menos duas cadeias cinemáticas independentes. A principal vantagem desse tipo de dispositivo é a sua elevada capacidade de carga e sua precisão de posicionamento. Porém, modelos convencionais de robôs paralelos apresentam espaço de trabalho extremamente reduzido quando comparados a robôs seriais. A adoção de cabos na estrutura cinemática de robôs paralelos atuados por cabos busca principalmente aproveitar das vantagens de robôs paralelos convencionais e reduzir algumas de suas desvantagens. Entre as diversas vantagens da alteração dessa configuração cinemática destaca-se principalmente a possibilidade de expansão do espaço de trabalho desses dispositivos para dimensões nunca antes imaginadas em robôs paralelos. Por outro lado, essa alteração de configuração resulta em um dispositivo muito mais complexo de ser modelado e controlado.

Objetivos

Robôs por cabos podem ser considerados uns dos dispositivos mais promissores da atualidade. Características como amplo espaço de trabalho e baixo custo fazem com que este equipamento seja extremamente interessante para aplicações como paletização e pick-and-place. Porém, esse dispositivo ainda não possui a popularidade que sua capacidade permite. O objetivo principal deste trabalho foi contribuir para a geração de conteúdo teórico sobre robôs por cabos visando principalmente auxiliar no projeto e adoção deste equipamento. Para tanto, foram desenvolvidas ferramentas teóricas que auxiliam o entendimento e aplicação dos robôs paralelos atuados por cabo para diferentes ambientes e tarefas. Por esse motivo, a capacidade do dispositivo suportar e exercer forças foi escolhida como tema deste trabalho. O método aqui proposto permite também que projetistas de robôs criem mapas de capacidade de força para orientarem seus clientes e utilizem tais mapas para otimizarem o projeto desses dispositivos. Outro aspecto a ser considerado,

com o método aqui proposto, é a avaliação da capacidade de força em tempo real, permitindo assim que o robô otimize comportamentos como sua geração de trajetória baseado em sua capacidade de força.

Metodologia

A capacidade de força é definida como a habilidade de um robô de exercer ou suportar forças diante de sua configuração cinemática e da capacidade de seus atuadores. Porém, como os cabos que compõem esses dispositivos são capazes apenas de realizarem forças unidirecionais e não compõe a cadeia cinemática do dispositivo quando não acionados. Nesse caso, dois conceitos foram utilizados para determinar a configuração do dispositivo e o modo de atuação da forças no mesmo. Primeiramente, robôs por cabos foram considerados como dispositivos intrinsecamente reconfiguráveis tendo sua configuração física sendo constantemente alterada de acordo com as ações que atuam na sua plataforma móvel. Nesse caso, o segundo conceito, da restrição exata, foi utilizado para determinar se a orientação da força externa é capaz de gerar um dispositivo estaticamente determinado capaz de suportar a ação proposta. Concluída a avaliação da configuração do dispositivo, a rotina de determinação da capacidade de força pode prosseguir. Nesse caso, um sistema inteligente busca automaticamente o melhor método para a solução do modelo estático do robô e posteriormente a definição da capacidade de força do dispositivo. Finalmente, a união dos conceitos aqui apresentados e organizados em um algoritmo com processos iterativos permitem a criação de mapas de capacidade de força e de mapas tridimensionais de espaço de trabalho e de trajetória de força. Para tanto, basta que sejam definidas as direções de interesse das ações na plataforma móvel do robô e também as possíveis posições da plataforma móvel.

Resultados e Discussão

O principal aspecto operacional de um robô é a sua capacidade de realizar tarefas. Nesse caso, para tarefas que demandam força é crucial que a capacidade de força do dispositivo seja conhecida. Nesse caso, o principal resultado deste trabalho é um método capaz de avaliar de forma precisa e rápida a capacidade de força de robôs planares atuados por cabos. Para ilustrar a adoção do método foram gerados mapas de capacidade de força de dispositivos com 2, 3 e 4 cabos. Também foram produzidos mapas de trajetória de força e do espaço de trabalho de força de robôs com dois cabos. Finalmente, os resultados do método aqui proposto foram comparados aos resultados propostos por Abdelaziz. Nesse caso, observou-se que o mapa de capacidade de força proposto por esse autor não avaliava completamente a determinação estática da plataforma como o método aqui proposto resultando em avaliações imprecisas da capacidade de força.

Considerações Finais

Segundo alguns autores, o potencial máximo de robôs paralelos atuados por cabos ainda não foram explorados. Eles afirmam que esses dispositivos ainda estarão presentes em diversas áreas, podendo até reescrever as regras de manipulação robótica. Porém, o crescimento dessa área está diretamente ligada aos resultados obtidos nas pesquisas desses dispositivos. Assim, a principal contribuição deste trabalho para a popularização desse dispositivo foi a definição de um método de avaliação de robôs por cabos capaz de definir de forma rápida e precisa a capacidade de força desses dispositivos baseado na teoria de mecanismos. A primeira tarefa alcançada foi a definição do modelo matemático do robô. Para tanto, cada cabo foi modelado como uma estrutura RPR e as condições de tracionamento tratadas como uma reconfigurabilidade natural do dispositivo. Nesse caso, o método de Davies foi aplicado para resolver o modelo estático do robô. Além disso, a plataforma móvel do equipamento foi analisada como um corpo livre que deveria ser exatamente restrita pelos cabos e forças externas para definir completamente a sua pose. Dois métodos de solução foram aplicados nesse projeto, o método de fator de escala e a otimização com restrições. No primeiro, as soluções foram obtidas sem um processo iterativo mas sua aplicação é restrita apenas para sistemas planares de dois cabos. Adicionalmente, a otimização com restrições é utilizada em situações com um número superior de cabos. Finalmente, o principal aspecto desse projeto foi a variação inteligente entre essas abordagens criando um precedente para utilização dessa abordagem em outros sistemas reconfiguráveis.

Palavras-chave: Robôs por Cabos. Capacidade de Força. Espaço de Trabalho. Estática. Método de Davies.

ABSTRACT

The development of robots allowed that several unhealthy activities, previously performed by humans, to be completely done by mechanical manipulators. As a result, the world economy has been reorganizing and human beings can concentrate on intellectual activities. Later, to amplify this effect, it is necessary robotic devices capable of performing the most different types of activities and that adapt to the most different economic situations. Cable driven parallel robots, the central theme of this work, are one of the most promising devices on this subject thanks to its many characteristics. Among them, the high dimension workspace, the low production cost and the fast winding of the cables stand out, allowing unique dynamic characteristics. Another significant aspect of this type of equipment is that the flexibility of the cables makes them more suitable for interactions with humans. However, even with all these qualities, several aspects of these devices are still open in academia. Among them, is the motivation of this work, which is the force capacity of these devices and, from this information, the definition of force capacity maps and the wrench-feasible workspace. The first aspect of this research was define the mathematical model that could translate all the nuances of this type of device. In this case, the greater complexity was the constant change in the number of actuated cables. Thus, in order for the mathematical model to be reasonable, it was necessary to treat the cable robot as a reconfigurable device and to establish laws that represented such reconfigurability. After summarize the possible planar models, it was needed to define methods that were able to establish the force capability of these manipulators. For this, the Davies method was associated to the scale factor method and the constrained optimization. An intelligent transition system varies the solution method according to the current device?s model. Finally, the method proposed by this work was defined and consolidated in an algorithm. The main steps of the method are the definition of all the possible robot's mathematical models, the establishment and iteration between all the actions to be applied in the end-effector and the solution of the force capability for each of the iteration steps using the appropriate mathematical model. After completing these steps, a power capacity map is defined. In addition to the definition of the method, force capability maps were obtained for planar robots with 2, 3 and 4 cables. Additionally, wrench-feasible workspace maps for 2 and 3 wire configurations were defined. This information allows an accurate assessment of the ability of these devices to perform tasks and follow trajectories involving force. Furthermore, a comparison was made between the results obtained

in this study and some studies in the literature. Finally, the proposed method was presented as more efficient when compared to methods without the smart switch, besides guaranteeing, through the concept of exact restriction, the pose of the robot's mobile platform.
Keywords: Cable Robots. Force Capability.Workspace. Statics. Davies Method.

LIST OF FIGURES

LIST OF TABLES

LIST OF ABBREVIATIONS

DE	Differential Evolution
DOF	Degree of Freedom
CDPR	Cable Driven Parallel Robot
CRPM	Completely Restrained Parallel Manipulator
CSPM	Cable-suspended parallel mechanisms
FCM	Fully-constrained mechanisms
IME	Instituto Militar de Engenharia
INRIA	Institute for Research in Computer Science and Automation
ITA	Instituto Tecnológico da Aeronaútica
IRPM	Incompletely Restrained Parallel Manipulator
MAV	Maximum Available Value
MIV	Maximum Isotropic Values
NIST	National Institute of Standards and Technology
RPR	Revolute Prismatic Revolute
RRPM	Redudantly Restrained Parallel Manipulator
UFSC	Universidade Federal de Santa Catarina
UFU	Universidade Federal de Uberlândia

LIST OF SYMBOLS

$[A_D]_{\lambda \times F}$ Matrix of Actions.

$[\hat{A}_N]_{\lambda.k \times C}$ Network of unitary actions matrix.

$[\hat{A}_{NP}]_{a \times C_N}$ Matrix containing the network unit action matrix?s columns corresponding to the primary variables.

$[\hat{A}_{NS}]_{a \times a}$ Matrix containing the network unit action matrix?s columns corresponding to the secondary variables.

$[B]_{l \times e}$ Fundamental circuit matrix built from coupling graph.

$[B_M]_{l \times F}$ Matrix of circuits-f.

c_i Degrees of constraint on relative motion imposed by joint i.

C_N Net degree of constraint.

C Gross degree of constraint.

f_i Degrees of relative motion permitted by joint i.

h Screw Pitch

j Number of joints in a mechanism, assuming that all joints are binary.

j_i Number of joints with i DoF.

λ Degrees of freedom of the space in which a mechanism is intended to function.

L Number of independent loops in a mechanism.

M Degrees of freedom of a mechanism.

$[M_D]_{\lambda \times F}$ Matrix of Motions.

$[\hat{M}_D]_{\lambda. \times F}$ Matrix of unitary Motions.

$[\hat{M}_N]_{\lambda.l \times F}$ Network unit motion matrix.

$[\hat{M}_{NP}]_{m \times F_N}$ Matrix containing the network unit motion matrix?s columns corresponding to the primary variables

$[\hat{M}_{NS}]_{m \times F_N}$ Matrix containing the network unit motion matrix?s columns corresponding to the secondary variables

n Number of links in a mechanism, including the fixed link.

n_c Number of cables.

n_d Number of degrees of freedom of a manipulator.

$\$$ Screw

$\$^M$ Twist

$\$^A$ Wrench

$[Q]_{k\times e}$ Fundamental cutset matrix built from coupling graph.

$[Q_A]_{\lambda.k\times C}$ Cutset-f Matrix.

ω Angular differential velocity

$\{\vec{\Psi}\}_{C\times 1}$ Vector containing magnitudes of wrenches

$\{\vec{\Psi}\}_{C_N\times 1}$ Vector containing magnitudes of the primary variables of the action analysis

$\{\vec{\Psi}\}_{a\times 1}$ Vector containing magnitudes of the secondary variables of the action analysis

v Translational differential velocity

τ Joint torques

CONTENTS

1 INTRODUCTION

This research proposes the force capability definition for planar cable driven parallel robots. This performance parameter is defined as the maximum force or torque that a manipulator is able to apply in the environment or it is able to support in static or quasi-static situations. Some applications of the force capability are the optimum robot design and the definition of robots' characteristics such as the force-feasible workspace and force capability maps.

1.1 CABLE DRIVEN PARALLEL ROBOTS

A parallel manipulator, as opposed to classical serial manipulators, is a closed-loop mechanism composed of an end-effector having n degrees of freedom and a fixed base, linked together by at least two independent kinematic chains. The main advantages of these devices are the load-carrying capacity and its good positioning accuracy. The main drawbacks of conventional parallel robots are their small workspace and the singularities that can appear during it's operation (MERLET; GOSSELIN, 2008).

Cable driven parallel robots are a special class of parallel mechanisms whose legs were replaced by cables. These devices were developed by Landsberger & Sheridan in 1985 to surpass some of the workspace limitations of traditional parallel robots. However, new challenges were created by this new configuration such as the need to avoid sagged cables. There are two main strategies to surpass this limitation. The parallel cable robot can be fully defined by its cables or by forces made at the robot end-effector (GOSSELIN, 2014).

One of the main characteristics of cable driven parallel robots is the possibility to change its workspace by just changing the length of the kinematic chains' cables. It can be easily done by coiling the tendons onto a drum. Since it can be coiled very fast, this type of robot has very high end-effector speeds and accelerations. Regarding the number of cables it is possible to be increased to modify the workspace, to carry higher loads or to increase safety due to redundancy (BRUCKMANN et al., 2008).

The first documented prototypes of working cable driven parallel robots were developed at the United States and Japan. According to Pott et al. (2013), the Robocrane (1989), developed for large scale manipulation by the National Institute of Standards and Technology (NIST) (ALBUS; BOSTELMAN; DAGALAKIS, 1992) appears to be the first prototype of

a cable driven parallel robot. Later, Falcon was developed by Kawamura (KAWAMURA et al., 1995) to be a fast pick-and-place robot, and Tadokoro et al. (1999) build a device to be a robotic mobile system to rescue victims of earthquakes. Lafourcade, Llibre and Reboulet (2002) implemented a cable driven parallel robot for motion generation in wind tunnels (Fig. 1).

Figure 1: Sacso - A cable driven parallel robot for Wind Tunnels. Available at Lafourcade, Llibre and Reboulet (2002).

Researchers at the German university of Duisburg-Essen (BRUCKMANN, 2010) developed a low weight prototype called Segesta to evaluate the kinematic, control and design studies. Later, the String-man robot, was developed at the German Institute Fraunhofer IPK. The main goal was to aid patients on rehabilitation focused in force control and safety. (SURDILOVIC; BERNHARDT, 2004). French researchers at INRIA developed a family of robots called Marionet that includes a small scale prototype for high speeds, a portable crane for rescue and components for personal assistance (MERLET, 2008). At China, researchers have developed the biggest cable robot of the world for positioning and orientation of a telescope reflector called FAST (Fig. 2) (DUAN et al., 2008).

Since 2006, the Fraunhofer Institute develops a family of robots called IPAnema for inspection, manipulation and assembly operations in medium and large scale (POTT; MEYER; VERL, 2010). According to the researchers, the main goal of this research is develop a device based on industrial level components to produce a result with high reliability and robustness, using the state of the art of motors, amplifiers and control components (POTT et al., 2013).

In Brazil, the development of cable robots has mainly been done in three universities. The Military Institute of Engineering (IME) and the

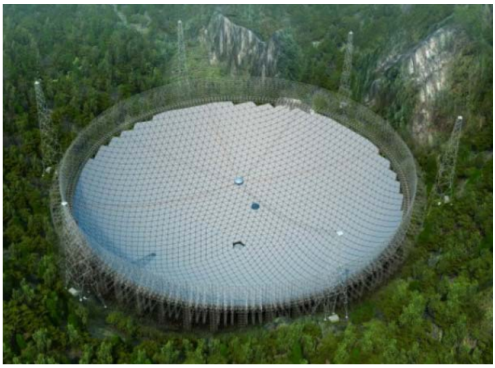

Figure 2: Cable driven parallel robot Fast. Available at Duan et al. (2008).

Federal Universities of Uberlandia (UFU) and Santa Catarina (UFSC). The SAMUCA prototype was developed by Travi (TRAVI, 2009) at IME. In UFU was developed a model for shoulder rehabilitation (NUNES, 2012). Finally, at UFSC, specially in the robotics laboratory several studies related to kinematic and static properties of cable driven parallel robots have been conducted by Muraro (2015) for the project: Reconfigurable Platform for bedridden patients.

Even with almost thirty years of development, cable robots still have not reached a commercial status. There are some issues of these devices that still needs to be addressed at research centres. One of the open issues is the force capability of these devices.

1.2 FORCE CAPABILITY

The creation of autonomous robots that are able to act in unpredictable environments has been a long-standing goal of robotics, artificial intelligence, and cognitive sciences. To do so, robots must be provided with a certain level of independence in order to face quick changes in the environment surrounding them (MEJIA; SIMAS; MARTINS, 2014).

In this case, strategies must be developed to allow robots to interact autonomously outside the predictability of research centres or universities facilities. In this context, when a physical contact with the environment is established, a process-specific force need to be exerted and this force has to be controlled against to the particular process preventing the overloading or damaging the manipulator or the objects to be manipulated (WEIHMANN et

al., 2011).

One of the main tools that have been continuously researched and developed along the last years in order to provide the robots with a high level of independence is the force capability. This tool is defined in an informal way as the capacity of a mechanical system to apply the quantity of force possible while it consumes the quantity of internal energy. This is one of the tools with the higher potential to optimize the performance of mechanical systems (MEJIA, 2016).

The interaction between a robot or a machine and its environment can be categorized in two classes. The first class is referred to unconstrained motion of non-contact tasks without any environmental influence on the robot. Several industrial applications such as pick-and-place, spray painting, gluing, and arc or spot welding belong to this category (MEJIA et al., 2015).

In contrast to the non-contact tasks, many complex advanced applications of robots and machines (packaging, assembling, or machining) require that the end-effector of such device to be coupled with other objects which can move, this kind of applications can be categorized as contact tasks.

The contact tasks can be furthermore divided into two subclasses: essential force tasks and compliant motion tasks. The first subclass requires the end-effector to establish a physical contact with the objects in the environment and exert a process-specific force. In these tasks, a synergy between the control of the end-effector position and interaction forces is required; some examples of this kind of tasks are deburring, roughing, bending, polishing, and others. In these tasks, the force has to be controlled in relation to the particular process in order to prevent overloading or damaging the tool or the objects to be manufactured (MEJIA; SIMAS; MARTINS, 2016).

In the second subclass, the tasks focus on the end-effector motion, which has to be realized close to the constrained surfaces, and it must be compliant (i.e., capable to reacting to the interaction forces). In this second subclass, the problem of controlling the robot is joined to the problem of accurate positioning (as in part-mating process). In the future of robotics, the interaction with the environment is fundamental and more and more tasks will include and require interaction.

In this research proposal we will focus on the contact task class and within this context, the force capability in robots will be studied. As a direct consequence, generalized methods to solve the force capability problem in planar parallel manipulators will be proposed.

In a formal way, the force capability of a robot, machine or mechanisms is defined as the maximum force that can be applied (or sustained) for a given pose, based on the limits of its actuators. The force capability of a

mechanical device is dependent on its design, posture, actuation limits and redundancies.

The wrench capability analysis is essential for the design and performance evaluation of mechanical devices. For a given pose, the end-effector is required to move with a desired force/moment or to sustain a specified wrench. Thus, the information of the joint torques that will produce such conditions could be investigated. This study is referred to as the inverse static force problem. An extended problem can be formulated as the analysis of the maximum wrench that the end-effector can apply into the wrench spaces.

The task space capabilities of a mechanical device to perform motion and/or to exert forces and moments are of fundamental importance in the design of robots. Their evaluation can be useful to determine the structure and the size of the device that best fit the designer's requirements or they can be used to find a better configuration or a better operation point for such a device to perform a given task.

Control of robots can conceptually be divided into position control and force control. Position control has been the main means of control for industrial and other existing robots. Although force control has been drawing attention of researchers and engineers since the early days of robot development, successful practical applications of force control are still quite few. In the future, however, the force control will be definitely needed in order to widen the application area and to increase dexterity of manipulators in industrial environments (for example, assembly, deburring, polishing, handling flexible parts, etc.) and also in non-industrial environments (hospital, home, town, space, etc. for service, maintenance, welfare, entertainment, etc.).

1.3 WORK PURPOSES

The main objective of this research is to define the force capability of cable driven parallel robots and by this means provide force capability and workspace maps. This objective will be achieved by some specific objectives that are:

- To define the statics of cable driven parallel robots through the Davies Method.
- To inspect conditions and factors that influences the force capability of the robot.
- To develop a method to determine the force capability of CDPRs.
- To define the force capability maps for cable driven robots.

- To determine the workspace maps based on the force capability.

1.4 JUSTIFICATION

Cable robots are one of the most promising devices in the present. It's unique features like large workspace and low cost makes it suited for a wide range of applications such as palletizing and pick-and-place. However, this robot still not as popular as it could be.

In this case, the motivation of this research is to contribute to the academic background regarding this robot and to provide theoretical tools that are able to help in the design and implementation of cable-driven parallel robots. To do so, the force capability, one of the main performance parameters of robots is analyzed.

Thus, the proposed method is meant to allow designers to create force capability maps during the robot project and also to improve the robot design using the method results. Additionally, robot buyers could also use the maps provided by the method to define the robot's ability to execute tasks and improve the tasks for the robot configuration. The high performance of the proposed method also allows real-time applications such as define the robot force capability of each point of a trajectory.

1.5 OVERVIEW OF THIS WORK

This work is divided into 7 chapters.

In Chapter 1, the concept of cable driven parallel robot is presented and some devices are analysed. The concept of *force capability* is also introduced alongside this work purposes and an overview.

In Chapter 2, the theoretical tools that are need to fully understand this work is presented. Thus, concepts such as the degree of freedom, the correspondence between mechanisms and graphs, the screw theory and the Davies Method are introduced.

In Chapter 3, a brief introduction about industrial robots is done starting with serial manipulators and showing the main advantages of cable robots. Finally, a classification of these devices and the solution of its static model is made.

In Chapter 4, the force capability is presented alongside a literature review on this subject. Further, some methods about the wrench polytopes analysis are presented alongside our proposed method. Furthermore, some case studies are showed to better explain our proposed method.

In Chapter 5, the concept of cable robots workspace is presented alongside some of the previous works on this subject. Further, a method is proposed to solve the *wrench-feasible workspace* and *trajectory* using the method that was proposed for the force capability.

In Chapter 6, a discussion is done regarding some results that are available in the literature and the ones that were obtained with the proposed method.

In Chapter 7, some conclusions and further works are presented. Thus, the performance of the method is reviewed and works such as the analyses of spatial robots are proposed as further works.

2 THEORETICAL TOOLS

This chapter presents some of the theoretical tools that are used in this work. Davies (1981) proposed a method to apply the Kirchhoff's circulation laws in the analyses of multi-loop kinematic chains. Its main purpose was to find a set of independent instantaneous screws associated with any two bodies in kinematic chains when the configuration of this chain is given. Thus, an analogy between electrical current (flow variable) and voltage (effort variable) with mechanical screw wrenches and motions, respectively, is proposed. This association allows to analyse separately the motion and the action of a set of coupled rigid bodies just by the means of graph and screw theory.

The following sections introduce some important concepts on mechanisms, graphs and screw theories. Further information can be found in the work of Cazangi (2008).

2.1 LINKS AND JOINTS

Rigid bodies are defined as material bodies whose deformation under stress is negligibly small. The use of rigid bodies makes the study of kinematics of mechanisms easier. However, for light-weight and high-speed mechanisms, the elastic effects of a material body may become significant and must be taken into consideration. The individual rigid bodies in a machine or mechanism are called *links*. *Joints* (Fig. 3) are elements that adds constraints to the relative motion between two members or *links* by connecting them. The relative motion permitted by a joint is governed by the form of the surfaces of contact between the two members. The surface of contact of a link is called a pair element. Two paired elements form a *kinematic pair* (TSAI, 2000).

Tsai (2000) classifies kinematic pairs according two main characteristics: the type of contact between the paired elements and the number of constraints. In the first classification, pairs are divided into *lower pairs*, when one element envelopes the other, and *higher pairs* when they have just a line or a point contact. The most common mechanical joints are presented in Fig. 3. The *revolute joint*, *R*, allows two links to rotate about an axis defined by the joint geometry, imposing five constraints on the paired elements.

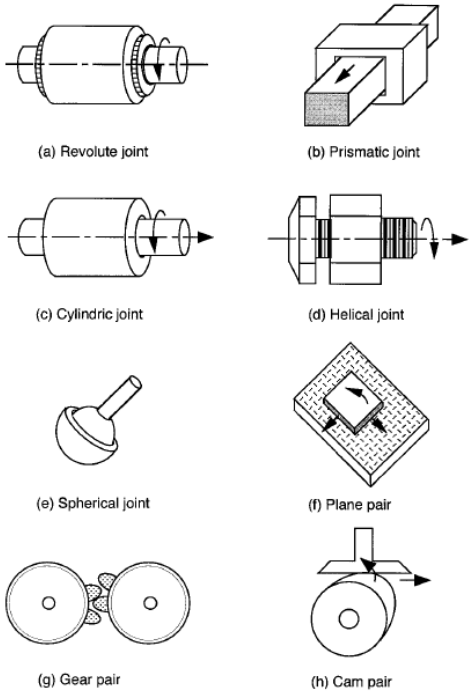

Figure 3: Some of the most popular mechanical joints. Available at Tsai (2000).

2.2 DEGREES OF FREEDOM

Degrees of freedom (DoF's) refer to the number of independent parameters required to completely specify the configuration of a mechanism in space, and perhaps is the first concern in the study of kinematics and dynamics of mechanisms. Except for some special cases, it is possible to define the degrees of freedom of a mechanism in terms of the number of links, number of joints, and types of joints incorporated in the mechanism by a general expression. Tsai (2000) defines the following parameters to facilitate the derivation of the degrees of freedom equation.

- c_i: degrees of constraint on relative motion imposed by joint i.
- F: degrees of freedom of a mechanism.

- f_i: degrees of relative motion permitted by joint i.
- j : number of joints in a mechanism, assuming that all joints are binary.
- j_i: number of joints with i DoF; namely, j_1 denotes the number of 1-DoF joints, j_2 denotes the number of 2-DoF's joints, and so on.
- L: number of independent loops in a mechanism.
- n: number of links in a mechanism, including the fixed link.
- λ: degrees of freedom of the space in which a mechanism is intended to function. For spatial mechanisms, $\lambda = 6$, and for planar and spherical mechanisms, $\lambda = 3$. λ is called the motion parameter.

Intuitively, the DoF's of a mechanism correspond to the DoF's of all the moving links subtracted by the degrees of constraint imposed by the joints. Since the total number of constraints imposed by the joints, according to Tsai (2000), is given by $\sum_{i=1}^{j} c_i$ the net degrees of freedom of a mechanism is

$$M = \lambda(n-1) - \sum_{i=1}^{j} c_i \tag{2.1}$$

The constraints imposed by a joint i and the degrees of freedom permitted by the joint are related by

$$c_i = \lambda - f_i \tag{2.2}$$

Substituting Equation 2.2 into Equation 2.1 yields to the *Chebychev-Grübler-Kutzbach* criterion:

$$M = \lambda(n-j-1) - \sum_{i=1}^{j} f_i \tag{2.3}$$

This criterion is valid only if the constraints imposed by the joints are independent and do not introduce redundant degrees of freedom. It is also possible to establish an equation that relates the number of independent loops to the number of links and number of joints in a kinematic chain. Tsai (2000) defines that a kinematic chain whose number of independent loops is increased from 1 to L has the difference between its number of joints and links increased by L-1, it yields to the *Euler's equation*:

$$\nu = j - n + 1 \tag{2.4}$$

Or, in terms of the total number of loops, we have

$$\tilde{L} = j - n + 2 \tag{2.5}$$

Combining Eq. 2.4 with Eq. 2.3 yields to the *loop mobility criterion*

$$\sum_{i=1}^{j} f_i = F + \lambda L \tag{2.6}$$

2.3 CORRESPONDENCE BETWEEN MECHANISMS AND GRAPHS

A *graph* consists of a set of *vertices* that are linked together by a set of *edges*. Graphs are denoted by the symbol G, the *vertex* by set V, and the edge by set E. We call a graph with v vertices and e edges a $G(v,e)$ graph. A *circuit* is denoted as a path of alternating vertices and edges, beginning and ending at the same vertex were each vertex appears once (TSAI, 2000).

A *tree* (T) is a connected graph that contains no circuits, with v vertices. According to Tsai (2000), any two vertices of T are connected by only one path and contains $(v-1)$ edges. The connection of any two non-adjacent vertices of T with an edge leads to a graph with one and only circuit.

A *spanning tree* (T) is a *subgraph* of the connected graph G that contain all its vertices. The edge set E of G can be decomposed into two disjoint subsets, called the arcs and chords. The arcs of G consist of all the elements of E that form the spanning tree T, whereas the chords consist of all the elements of E that are not in T. The union of the arcs and chords constitutes the edge set E (TSAI, 2000).

In general, the spanning tree of a connected graph (G) is not unique. The addition of a chord to a spanning tree forms precisely one circuit. A collection of all the circuits with respect to a spanning tree forms a set of independent loops or fundamental circuits. Figure 4a shows a $(5,7)$ graph G, Figure 4b shows a spanning tree T, and Figure 4c shows a set of fundamental circuits with respect to the spanning tree T (TSAI, 2000).

A *cutset* is a edge set, that separates the graph into two sub-graphs when it is removed. A *fundamental cutset* (*cutset-f*) is obtained by a single edge of the graph tree and a set of chords. In contrast, the *fundamental circuit* (*circuit-f*) is obtained by a single chord and a set of tree branches. In addition the *cutsets-f* may be represented by a *Cutset-f Matrix* denoted by $[Q]_{k\times e} = [q_{i,j}]$ composed by the following rules (CAZANGI, 2008).

- $q_{i,j} = 1$ if e_i belongs to the *f-cutset* k_i and has the same orientation that the tree branch that defines it.
- $q_{i,j} = -1$ if e_i belongs to the *f-cutset* k_i and has an opposite orientation

compared to that the tree branch that defines it.

- $q_{i,j} = 0$ if e_i does not belong to the *cutset-f* k_i.

In the same manner, the *circuits-f* may be represented by a *circuits-f matrix* denoted by $[B]_{l \times e} = [b_{i,j}]$ composed by the following rules defined in Cazangi (2008).

- $b_{i,j} = 1$ if e_i belongs to the same *circuit-f* l_i and has the same orientation that the chord that defines it.
- $b_{i,j} = -1$ if e_i belongs to the same *circuit-f* l_i and has an opposite orientation with respect to the chord that defines it.
- $b_{i,j} = 0$ if e_i does not belong to the *cutset-f* l_i.

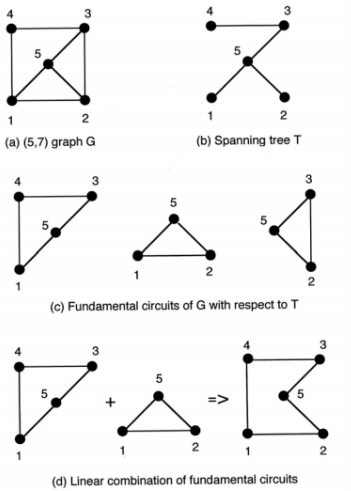

Figure 4: A spanning tree and the corresponding fundamental circuits. Available at Tsai (2000).

2.3.1 Structural Analysis

Structural analysis studies the nature of connections among the members of a mechanism. Since the topological structure of a kinematic chain can be represented by a graph, many useful characteristics of graph theory can be

applied to analyse kinematic chains. Table 1, by Tsai (2000), describes the correspondence between the elements of kinematic chains and graphs.

Table 1: Correspondence between mechanisms and Graphs. Available at (TSAI, 2000)

Graph	Symbol	Mechanism	Symbol
Number of vertices	v	Number of links	n
Number of edges	e	Number of joints	j
Number of vertices of degree i	v_i	Number of links having i joints	n_i
Degree of vertex i	d_i	Number of joints on link i	d_i
Number of independent loops	L	Number of independent loops	L
Total number of loops $(L+1)$	$\tilde{L}$	Total number of loops $(L+1)$	$\tilde{L}$
Number of loops with i edges	L_i	Number of loops with i joints	L_i

2.4 CONCLUSIONS

In this chapter, some fundamental concepts regarding *mechanism and machine theory* were analysed, such as the concept of degrees of freedom, informations about links and joints and the graph theory. Thus, the statics and kinematics behaviour of mechanisms can be fully understood. To do so, the *screw theory* alongside the *Davies' method* is introduced. In this case, a new geometric element called *screw* allows the representation of the instantaneous state of motions and actions of rigid bodies in space. Further, the concept of *screw wrench* and *screw twist* alongside the adaptation of *Kirchhoff's circuit laws* for mechanics were presented, and applied to fully define all actions and moments in a mechanism. Finally, the use of this well substantiated and traditional concepts will allow to increase the reliability and robustness of the proposed method.

3 BIBLIOGRAPHIC REVIEW

The *Robotics Institute of America* defines a robot as a "re-programmable multi-functional manipulator designed to move materials, parts, tools, or specialized devices, through variable programmed motions for the performance of a variety of tasks". Although most people perceive robots anthropomorphically, today's industrial robots are mechanical manipulators somewhat humanoid in appearance. Robot manipulators were first introduced in the late 1940s to handle hazardous materials and to work in space exploration and for flexible automation (TSAI, 1999).

Robots can be categorized according to several classifications such as working purposes, operation environment and others. Here, since our main focus is to introduce a parallel architecture, they will be classified based on its kinematic structure. In this case, there are three main classes serial, parallel and hybrid manipulators.

3.1 SERIAL MANIPULATORS

A serial chain is a sequence of links and joints that begins at a base and ends with a end-effector. Currently, serial manipulators, like the one shown in Fig. 5, is based on a serial kinematic chain and are the most common type of manipulator used in robotics, mainly because its large workspace and simple operation. However, there are some drawbacks, such as high energy consumption and low payload to weight ratio.

Figure 5: Serial Robot Kuka IIWA. Available at Cobots (2018)

According to Verhoeven (2004), the energy consumption of these devices is rather high because each actuated joint has to carry not only the load, but also all the subsequent links with their actuators. Further, the capability of handling large masses is limited since heavy loads require stronger links and this increases energy consumption even further. In fact, in most manufacturing applications the payload, the robot capacity to carry weights, is quite small when compared to the mass of the whole manipulator.

Moreover, high velocities and accelerations can be easily achieved, especially when revolute joints are employed. Thus, links act as levers and therefore the end-effector generally moves faster than the joints. High precision operation is possible, especially in small-scale applications (workspaces up to about 1 m).

Verhoeven (2004) also addresses problems with large-scale operation. According to him, the leverage effect of long links increases substantially the torque on actuated joints whereas the bending of links and vibrations of large amplitude affects automatized/precise motions.

Contrasting, tendon-driven serial manipulators (Fig. 6), whose actuators are fixed, are considerably more energy efficient. However, in three-dimensional applications it is very difficult to guide the tendons around joints. Therefore, this concept is used in practice mainly for planar systems (VERHOEVEN, 2004).

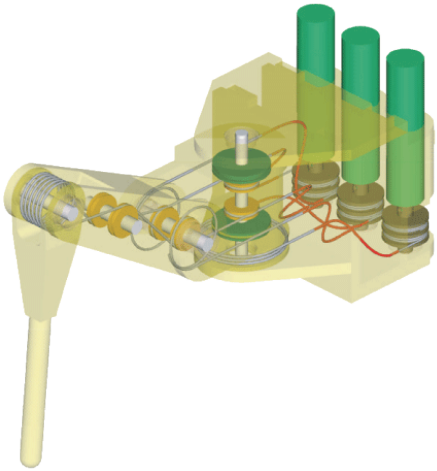

Figure 6: Tendon-driven Serial Manipulator. Available at Yin and Bowling (2018)

3.2 PARALLEL ROBOTS

According to Merlet and Gosselin (2008), a parallel manipulator can be defined as a closed-loop mechanism composed of an end-effector having n degrees of freedom and a fixed base, linked together by at least two independent kinematic chains, commonly called legs or limbs of the manipulator. In 1947, Gough established its basic principles allowing positioning and orientation of the moving platform to test tire wear and tear. However, early in 1928, an example (Fig. 7) of such structure was patented by Gwinnett (1931) to be used as a platform for a movie theater.

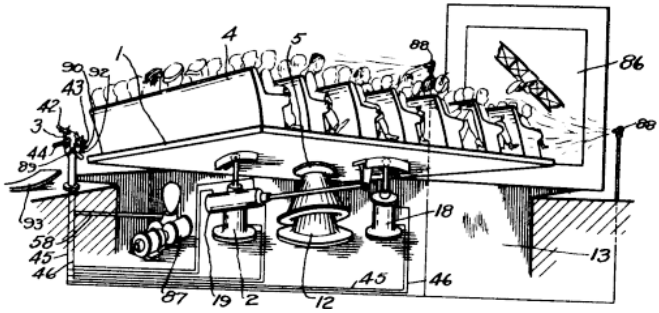

Figure 7: Gwinnett (1931) platform for movie theater.

Gough (1956) prototype (Fig. 8) was based on a hexagonal platform whose vertices are all connected by spherical joints to the robot limbs. A linear actuator allows the modification of the total length of the moving links (legs) that were connected to the base by a universal joint. Stewart (1965) suggested the use of such structure for flight simulators and the Gough mechanism is sometimes referred to as *Stewart platform*. The same architecture was also concurrently proposed by *Kappel* as a motion simulation mechanism (MERLET; GOSSELIN, 2008).

According to Gosselin (2014), the mechanical properties of parallel mechanisms make them most appropriate for tasks that require large payload to weight ratios or very demanding dynamic trajectories (e.g. high-speed robots). Indeed, while the payload to mass ratio is typically smaller that 0.15 for serial 6R industrial robots, can be larger than 10 for parallel structures, allowing them to operations such as machining (Fig. 9).

Further, it is well-known in structural engineering that designs involving links that are subjected to only tension and compression constitute an optimal use of materials. Thus, many of the most successful designs of par-

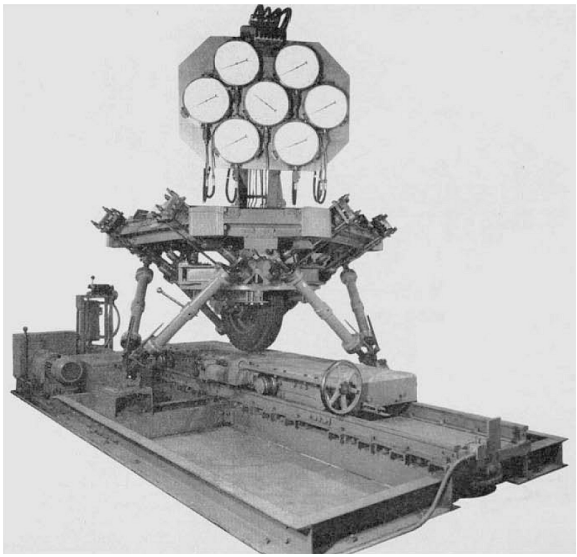

Figure 8: Gough (1956) parallel manipulator for test tires.

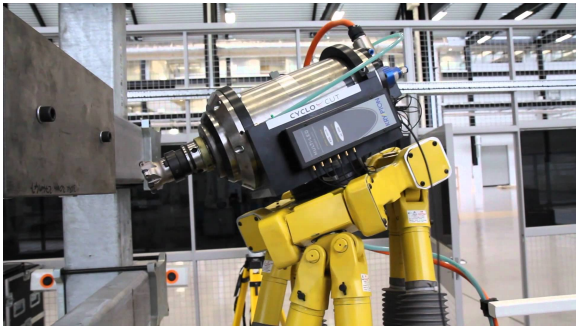

Figure 9: Stewart platform for machining. Available at AMRC (2018)

allel mechanisms involve some links that are subjected to only tensile and compressive loads. Moreover, it is only natural to extend the reasoning one step further and consider parallel mechanisms that involve members solely in tension, thereby leading to the concept of cable-driven parallel mechanisms - also referred as tendon-driven parallel mechanisms - introduced by Landsberger (1985) and Miura, Furuya and Suzuki (1985) (GOSSELIN, 2014).

According to Irvine and Irvine (1992), cables are flexible elements

that are able to support very large tensile loads per unit weight, representing a more effective use of materials compared to struts, which explains why they have been employed in construction and in machines since antiquity. Cable-driven parallel robots (CDPR) combine the principles of parallel mechanisms with the properties of cables, leading to potentially very effective mechanisms. Moreover, some of the main advantages of these devices are:

- They can have large workspaces since huge amounts of cables can be wound on spools and the weight of the robot limbs are incredibly small compared to rigid links.
- Very energy efficient since the actuators are fixed, the payload is subdivided between actuators and the robot legs are light.
- They are appropriate to handle very heavy loads, like cranes and the wound speed allows them to achieve very high accelerations and velocities.
- They can be designed in extremely large scale (up to several kilometers as the works of Duan et al. (2008)) as well as in micro-scale applications.
- Unlike in the case of cranes, motion is highly predictable and can be controlled without manual interaction.

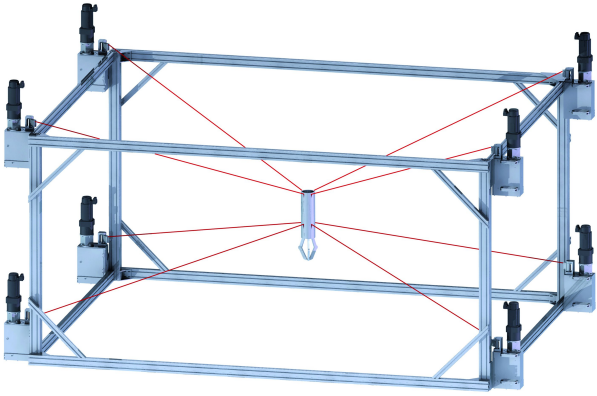

Figure 10: Ipanema Cable Robot. Available at Pott et al. (2013)

On other hand, some theoretical questions about cable-driven parallel robots remains unanswered and have been addressed by many researchers. Verhoeven (2004) enumerates some of them:

- The robot stiffness, since cables are much more compliant than rigid links;

- The collision of cables with each other, with the load or with the framework;

- The workspace complexity due mainly to the unidirectional behaviour of the cable limbs;

- The optimal distribution of tension between tendons, especially in highly redundant systems.

3.3 CLASSIFICATION

Cable robots were first classified by Ming and Higuchi (1994) who divided them into two main classes the *Completely Restrained Parallel Manipulator - CRPM* and the *Incompletely Restrained Parallel Manipulator - IRPM*. Ten years later, Verhoeven (2004) divided the CRPM class in two, adding the category *Redundantly Restrained Parallel Manipulator - RRPM*. The classification is made based in the difference between the number of cables n_c and the number of degrees of freedom n_d of the manipulator:

- IRPM (Incompletely Restrained Parallel Manipulator): In the IRPM configuration the number of cables is inferior to the number of degrees of freedom, thus they cannot completely define the position of the mobile platform, requiring the presence of external forces at the end effector.

$$n_c \leq n_d \tag{3.1}$$

- CRPM (Completely Restrained Parallel Manipulator): The CRPM has the exact amount of cables that are needed to fully constrain the end effector. In this case, no external force is needed to define the platform position.

$$n_c = n_d + 1 \tag{3.2}$$

- RRPM (Redundantly Restrained Parallel Manipulator): The RRPM has a number of cables that is bigger than the amount needed to completely restrain the parallel manipulator. Thus, during operation some of its cables may remain sagged or tightening themselves.

$$n_c < n_d + 1 \tag{3.3}$$

Table 2: Classification of the cable driven mechanisms according to its controllable degrees of freedom. (VERHOEVEN, 2004).

Class	DoFs	Type of Movement
1T	1	Linear movement of a point.
2T	2	Planar movement of a point.
1R2T	3	Planar movement of a body.
3T	3	Spacial movement of a point.
2R3T	5	Spacial movement of a bar.
3R3T	6	Spacial movement of a body.

Verhoeven (2004) also classifies the cable driven parallel robots according to the number of controllable degrees of freedom and the type of moment that the end effector is able to perform, as shown in Tab. 2 and Fig. 11.

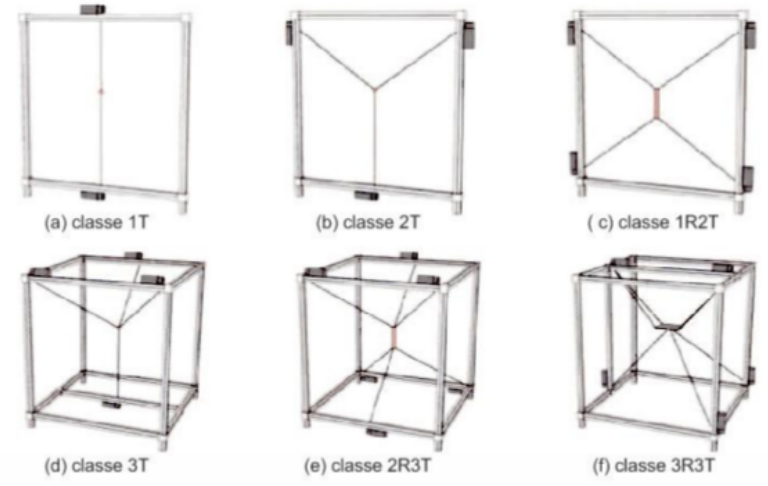

Figure 11: Verhoeven (2004) classification of Cable Driven Parallel Robots

The works of Gosselin (2014) also propose a classification method for cable driven parallel robots. There, the author divides them into two classes, *fully-constrained mechanisms - FCMs* and *cable-suspended parallel mechanisms - CSPMs*. In this case, the CSPMs (Fig. 12a) requires the presence of external forces in the end effector (*mainly gravity*) to fully define its posture. In contrast, FMCs (Fig. 12b) can fully define its posture just by

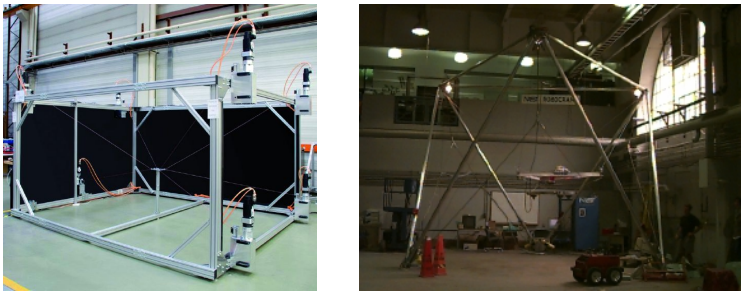

(a) *Fully-constrained mechanisms* (b) *Cable-suspended parallel mechanism*

Figure 12: Gosselin (2014) classification demonstration.

its own configuration since they are designed in a way that allows its cables to pull themselves.

3.4 CONCLUSIONS

The presence of robots in the industrial environment is constantly increasing. However, most of these devices are serial robots with rigid links with many drawbacks such as energy consumption and reduced workspace. Cable Robots, such as the *skycam* (CONE, 1985), can allow the development of systems in a scale that was never thought before in a significantly reduced price. Thus, to increase the popularity of these devices in the industrial environment some advances in the academic field must be done. To do so, this chapter presented an introduction about this device, a classification proposal for some of the available CDPRs and the solution of the robot static model.

4 FORCE CAPABILITY OF CABLE ROBOTS

Force capability is defined as the robot ability to exert or support a specified force according to its kinematic configuration and the actuators maximum torque/force. On cable robots, the unidirectional actuation leads to some issues in the determination of its force capability. Thus, before the capacity definition, the behaviour of the robot's mobile platform is analysed alongside each possible actuation. In this case, the concept of *exact constraint*, proposed by Blanding (1992), is used to define poses where the mobile platform is able to perform or support forces.

Moreover, the concepts of instantaneous twist and wrench capability are essential for the design and performance evaluation of serial and parallel manipulators. According to Firmani et al. (2008), an instantaneous twist is a screw quantity that contains both angular and translational velocities of the end-effector, i.e., $V = \{\gamma^T; v^T\}^T$. Whereas, a wrench is a screw quantity that contains the forces and moments acting on the end-effector, i.e., $F = \{f^T; m^T\}^T$. For a given pose, the required task of the end effector is to move with a desired twist and to sustain (or apply) a specific wrench (FIRMANI et al., 2008). These kinematic conditions are achieved with corresponding velocities ($\dot{q}$) and joint torques (τ) respectively. The relationship between the task and joint spaces is defined by the well known linear transformations, where J is defined as the *Jacobian matrix*:

$$\dot{x} = \mathbf{J}\dot{q} \tag{4.1}$$

$$\tau = \mathbf{J}^T F \tag{4.2}$$

In addition, an extended problem can be formulated as the analysis of the maximum twist or wrench that the end-effector can perform in the twist or wrench spaces, respectively. Thus, the knowledge of maximum twist and wrench capabilities is an important tool for achieving the optimum design of manipulators (FIRMANI et al., 2008).

For instance, according to Mejia (2016), by being able to graphically visualize the twist and wrench capabilities, comparisons between different design parameters, such as the actuator force capabilities and the dimensions of the links, can be explored. Also, the performance of an existing manipulator can be improved by identifying the optimal capabilities based on the configuration of the branches and the pose of the end-effector (FIRMANI et al., 2008). This work focus on the wrench capabilities of planar manipulators actuated by cables.

4.1 FORCE CAPABILITY INFLUENCE FACTORS IN MANIPULATORS

According to Mejia (2012), the manipulator force capability is influenced by a series of factors, among which the most important are:

- The type of the applied wrench;
- Kinematic redundancy;
- Environment possible reactions;
- The manipulator working mode;
- Manipulator singularities;
- The actuators capacities and limitations;
- Geometrical characteristics and configuration of the manipulator;
- Manipulator stiffness.

In this case, the concept of manipulator stiffness is formalized as the relation between the forces and the deformations caused in the end effector. A bigger stiffness will lead to less deformation, considering the same forces and moments acting in the end effector (SALISBURY, 1980).

Weihmann (2011) shows a study about the influence of such factors in the force capability of manipulators, using practical examples and simulations of two planar manipulators. The author also exemplifies how different configurations for the same contact point can be achieved by the use of kinematic redundancy.

Nokleby et al. (2005) determines that the force capability of a manipulator is defined by its less powerful actuator, subject to actuation saturation. Thus, after the definition of the less powerful joint, the maximum torque/force is applied in this joint and, by equilibrium equations, the interaction actions among the manipulator and the environment is defined (MEJIA, 2012).

4.2 PERFORMANCE INDICES

According to Gosselin and Angeles (1991), an enormous amount of performance indices were formalized in the literature, but most is focused in kinematics of manipulators. Further, Mejia (2012) elucidates that performance indices for force capability of manipulators are presented by Gosselin and Jean (1996) and Finotello et al. (1998).

For Mejia (2012), *performance indices* aims to provide direct information about specified manipulators characteristics. Thus, in the development phase, *indices* are used as reference for topology, geometry and constructive characteristics of manipulators. Further, in operational phase, the *performance indices* can be used to define a proper posture and distribution of forces and torques in actuators (GOSSELIN; JEAN, 1996; FINOTELLO et al., 1998).

For Finotello et al. (1998), manipulability is the capability of a manipulator to perform a specified task with a known configuration and aims to characterize the kinematic condition of a manipulator. Further, the concept of manipulability was extended to statics, introducing the force ellipsoid, the most popular *static performance index* in literature. Furthermore, *force ellipsoids* were used to define *force capability* quantitative measures of manipulators.

Further, for Mejia (2012), the concepts of *maximum available value* (MAV) and *maximum isotropic values* (MIV) are also popular *performance indices* in statics. In this case, MAV is the maximum force or moment that a manipulator can apply in any direction and MIV as the maximum value of force or moment that the manipulator can exert in all possible directions.

Finotello et al. (1998) and Nokleby et al. (2005) treat the forces and moments separately, leading to different values of MAV and MIV. In this case, the nature of actions between the manipulator and the environment are characterized by the terms *strong sense* and *weak sense*. Thus, for forces, the *strong sense* is obtained with zero moments. Likewise, in the *weak sense*, moments can assume any value. Further, for *moments*, a similar concept is applied with forces being zero or assuming any value.

Firmani et al. (2008) defines some *performance indices* for parallel manipulators in a specified position using the concepts of MAV and MIV as follows:

- **Maximum force with a prescribed moment** (F_{app}^{pm}): is the maximum force that a manipulator is able to apply in a direction, considering a specified moment. If the value of the moment is zero, the concept of F_{app}^{pm} is equal to the MAV in the *"strong sense"*.
- **Maximum isotropic force with a prescribed moment** (F_{iso}^{pm}): is the maximum force that a manipulator is able to apply in all directions, considering a specified moment. If the value of the moment is zero, the concept of F_{iso}^{pm} is equal to the MIV in the *"strong sense"*.
- **Maximum allowable force** (F_{app}^{mr}): is the maximum force that the manipulator can apply in a direction with an associated moment. Thus, it is similar to the concept of MAV in the *"weak sense"*.

- **Maximum allowable isotropic force** (F_{iso}^{mr}): is the maximum force that the manipulator is able to apply in all directions with an associated moment. Thus, it is similar to the concept of MIV in the *"weak sense"*.
- **Maximum moment with a prescribed force** (M_z^{pf}): is the maximum moment that the manipulator can apply, considering a specified force.
- **Maximum moment with a prescribed maximum isotropic force (M_z^{if}):** is the maximum moment that the manipulator can apply, considering a maximum isotropic force.
- **Maximum moment with a prescribed maximum force (M_z^{rf}):** is the maximum moment that the manipulator can apply, considering a maximum force.
- **Maximum moment with a free force (M_z^{mr}):** is the maximum moment that the manipulator can apply, considering a free force.

4.3 LITERATURE REVIEW ON THE WRENCH CAPABILITY

According to Mejia (2016), the measurement of robots manipulating ability was first introduced by Yoshikawa (1985), where the velocity and force manipulability ellipsoids were defined. Currently, three different approaches for determining force capabilities have been proposed in the literature: constrained optimization, wrench ellipsoid and wrench polytope (FIRMANI et al., 2008).

4.3.1 Constrained Optimization

The constrained optimization approach, in general, involves an objective function that maximizes either the magnitude of the force (F) or the moment (M_z), one equality constraint ($F = \mathbf{J}^{-T}\tau$) and a set of inequality constraints ($\tau_{i_{min}} \leq \tau_i \leq \tau_{i_{max}}$), indicating the actuator output capabilities.

Mejia (2016) summarizes some previous studies with this approach. According to him, Kumar and Waldron (1988) investigated the force distribution in redundantly-actuated closed-loop kinematic chains and concluded that there would be zero internal forces using the Moore-Penrose pseudo-inverse solution. Tao and Luh (1989) developed an algorithm to determine the minimum torque required to sustain a common load between two joint-redundant cooperating manipulators. Nahon and Angeles (1992) described the problem of a hand grasping an object as a redundantly-actuated kinematic chain, by

minimizing the internal forces in the system using quadratic programming (QP).

Further, Weihmann et al. (2011) and Mejia, Simas and Martins (2014) proposed methodologies to evaluate the wrench capability of planar parallel manipulators using differential evolution algorithms (DE). Buttolo and Hannaford (1995) analysed the force capabilities of redundant planar parallel manipulator. Torques were optimized using the $\infty - norm$ resulting in higher force capabilities when compared to the pseudo-inverse solution.

Nokleby et al. (2005) developed a methodology to optimize the force capabilities of redundantly-actuated planar parallel manipulators using an n-norm, for large values of n, and a scaling factor. After, Nokleby et al. (2007) used these methods to obtain results for 3-RRR, 3-RPR and 3-PRR parallel architectures with redundant and non-redundant actuation. Furthermore, Zibil et al. (2007) implemented this approach to spatial parallel manipulators.

According to Mejia (2016), in general, constrained optimization methods, used as primary tool are usually slow due to the numerical nature of the algorithm and the inaccuracies due to the existence of local minima. Based on these limitations, in this work, two new approaches to solve the wrench capability problem are proposed as an attempt to reduce the time and effort needed to solve such a problem avoiding simultaneously the use of optimization algorithms or iterative processes. The method proposed by Mejia (2016) are based on the classic scaling factor method and on classical gradient-based optimization methods.

First, some improvements are proposed on the classic scaling factor method proposed by Nokleby et al. (2005) in order to avoid the use of an optimization algorithm. These improvements result in the definition of a modified scaling factor method that solves the wrench capabilities problem in an easier, faster and more direct way. When used in conjunction with the Davies method, the modified scaling factor method proposed by Mejia (2016) constitutes a powerful tool used to solve the wrench capability problem.

4.3.2 Wrench ellipsoid

According to Firmani et al. (2008), the *wrench ellipsoid* approach is based on bounding the actuator torque vector by a unit sphere $\boldsymbol{\tau}^T\boldsymbol{\tau} \leq 1$. Thus, the torques are mapped into the wrench space with Eq. 4.3, yielding a force ellipsoid $\mathbf{F}^T\mathbf{J}\mathbf{J}^T\mathbf{F} \leq 1$. However, Firmani et al. (2008) define this approach as an approximation because joint torques are normalized ($\boldsymbol{\tau}^T\boldsymbol{\tau} \leq 1$), yielding a hypersphere in the torque space. Thus, the correct model of the joint torques/forces must be an *m*-dimensional parallelepiped in the torque/force

space due to the nature of extreme torque capabilities of each actuator.

$$\boldsymbol{\tau} = \mathbf{J}^T \mathbf{F} \tag{4.3}$$

Thus, Mejia (2012) defines the *wrench ellipsoid* as a graphical representation of the relation between manipulator actuation and resultant actions in the end effector.

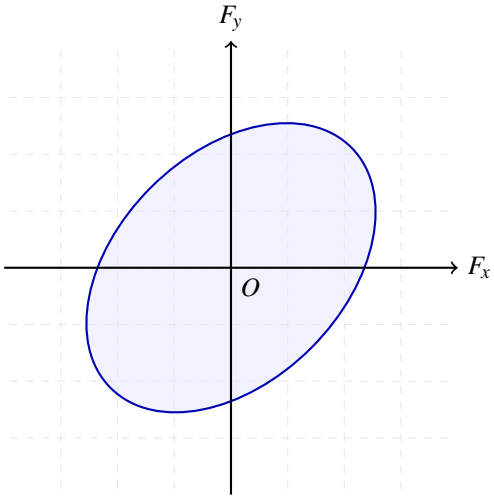

Figure 13: Force ellipsoid

Further, since the *ellipsoid* depends of the *Jacobian matrix*, each new manipulator configuration leads to a new *ellipse*. Furthermore, Weihmann (2011) summarize some considerations regarding the application of *force ellipsoids*:

- They are applied only when the manipulator presents only one joint type. In this case, mapping of manipulators with two or more types of joints would present dimensional inconsistency.
- They do not evaluate the links weight. Thus, the torques that are needed to equilibrate the gravitational forces are neglected, which can lead to incorrect results.
- They do not consider restrictions in the maximum manipulators torque. Thus, even normalizing the maximum torque of the most robust unit joint, some points of the torque maps could not be reached and,

consequently, the *force ellipse* does not represent accurately the real condition.

- Unitary norm excludes the possible combinations of the mapping torques. Thus, if the considered joints possesses the same torque capability, in the bi-dimensional cases the torques should be represented by a square and not a circle.

Even with all restrictions the *wrench ellipsoid* provides directions indicatives where the manipulator possesses the major mechanical advantages. Thus, these informations can be useful to find optimized solutions for the application of forces and moments limits. Further, in the presence of kinematic and actuation redundancy, its applicability is limited because does not provide information such as, from an initial configuration, how to improve the force capability for a specified direction through changes in the posture of the manipulator or how to efficiently distribute the torques in the actuators (GOSSELIN; SEFRIOUI, 1991).

4.3.3 Wrench polytope

According to Firmani et al. (2008), *wrench polytope* approach considers the complete region in which the actuator can operate and is compared to the *wrench ellipsoid* in Fig. 14. Thus, assuming a manipulator with two actuated revolute joints whose extreme capabilities are $\tau_{i_{ext}} = \pm 1$ Nm, for $i = 1, 2$, Fig. 14a describes the generation of an ellipse as a result of mapping a circle and Fig. 14b shows the generation of a polygon (in general, a polytope) as a result of mapping a square.

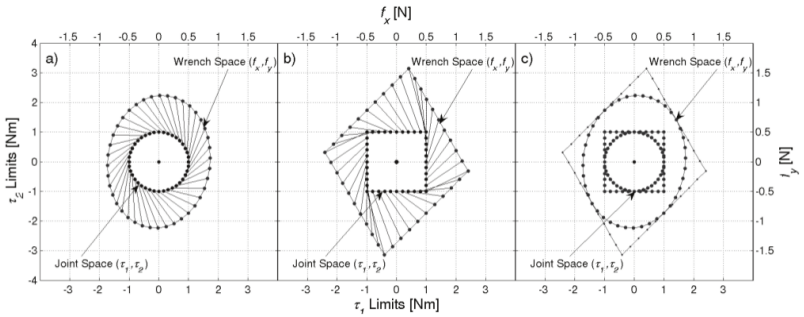

Figure 14: Mapping of ellipsoids and polytopes from the joint space the task space. Available at Firmani et al. (2008).

Further, the inner circle and the inner square of Fig. 14a and 14b, describe the torque limits in the torque space, respectively (bottom and left axes); whereas, the outer ellipse and polygon describe the wrench capabilities in the wrench space (top and right axes). Furthermore, the lines that connect the inner to the outer shapes illustrate the linear transformation. Finally, Fig. 14c shows how the circle and ellipse are inscribed within the square and polygon, respectively.

In general, according to Firmani et al. (2008), each actuator torque/force defines an orthonormal axis in $\mathbb{R}^m$. The extremes of each torque constrain the torque/force space with a pair of parallel planes along each axis. Thus, an m-dimensional parallelepiped is obtained by pairs of parallel planes which bounds the feasible region where the manipulator can operate. A linear transformation, such as the equation of the *forward static force*, maps vector $\boldsymbol{\tau}$ from $\mathbb{R}^m$(joint torque space) to $\mathbb{R}^n$ (wrench space).

4.4 WRENCH POLYTOPE ANALYSIS

4.4.1 Joint space parallelepiped

According to Firmani et al. (2008), the i^{th} joint torque variable, which is bounded by $\tau_{i_{min}}$ and $\tau_{i_{max}}$, can be represented in the joint torque space as two parallel planes in $\mathbb{R}^m$, being n the dof of the task space coordinates and m the number of actuated joints. Thus, with m joints, there are $2m$ planes or m pairs of parallel planes, whose combination forms an m-dimensional parallelepiped yielding the region of joint torque capabilities. Further, if all the torque capabilities were equal, the m-dimensional parallelepiped would result in a hypercube. Also, if the magnitude of the extreme torques were equal, i.e., $|\tau_{i_{min}}| = |\tau_{i_{max}}|$, the parallelepiped would be centro-symmetric; otherwise it would be skewed. A vertex of the m-dimensional parallelepiped defines the intersection of m extreme torque planes. Thus, a vertex occurs when all joint torques are at their extreme capabilities, i.e.,

$$v_j = \begin{bmatrix} \tau_{1_{ext}} & \tau_{2_{ext}} & \cdots & \tau_{1_{ext}} \end{bmatrix} \tag{4.4}$$

where $\tau_{i_{ext}}$ denotes the extreme capabilities of the i^{th} actuator, i.e., $\tau_{i_{min}}$ or $\tau_{i_{max}}$. According to Firmani et al. (2008), the total number of vertices(v_{T_m}) in the m-dimensional parallelepiped is $v_{T_m} = 2^m$.

4.4.2 Linear transformation

According to Firmani et al. (2008), Visvanathan and Milor (1986) investigated problems involving the mapping of a parallelepiped under a linear transformation. Further, Firmani et al. (2008) propose a linear transformation from $\mathbb{R}^m$ to $\mathbb{R}^n$, such as $F = \mathbf{J}^{-T}\tau$, to obtain a polytope from a m-dimensional parallelepiped. Furthermore, an n-dimensional convex polytope is bounded by $(n-1)$-dimensional facets or hyperplanes, e.g., linear edges in $\mathbb{R}^2$ bounding a polygon or planar facets in $\mathbb{R}^3$ bounding a polyhedron. Thus, a polytope $\mathbf{P}$ can be completely characterized by mapping all the vertices of the parallelepiped and enclosing them in a convex hull, i.e.,

$$\mathbf{P} = convh\left\{\mathbf{J}^{-T}v_j, j = 1, \cdots, 2^m\right\} \tag{4.5}$$

where *convh* detones a convex hull operator which encloses all the extreme points forming the feasible region of the torque space in the wrench space. Finally, the total number of vertices in the polytope (v_{T_n}) depends on the dimension of the two spaces (FIRMANI et al., 2008).

4.4.3 Non-redundant planar manipulators

According to Firmani et al. (2008), the number of vertices in the polytope, for non-redundant manipulators ($n = m$), is equal to the number of vertices in the m-dimensional parallelepiped, i.e., $v_{T_n} = v_{T_m} = 2^m$, and the vertices of the polytope are the image of the vertices of the m-dimensional parallelepiped, i.e.,

$$p_j = \mathbf{J}^{-T}v_j \tag{4.6}$$

where p_j and v_j are the vertices of the polytope and parallelepiped, respectively. Further, according to Firmani et al. (2008), the linear transformation also makes the edges and facets of the polytope as the corresponding image of the edges and facets of the m-dimensional parallelepiped. Thus, for planar parallel manipulator the vertices of the wrench polytope are found as follows:

$$\begin{bmatrix} f_x \\ f_y \\ m_z \end{bmatrix} = \begin{bmatrix} \gamma_{1,1} & \gamma_{1,2} & \gamma_{1,3} \\ \gamma_{2,1} & \gamma_{2,2} & \gamma_{2,3} \\ \gamma_{3,1} & \gamma_{3,2} & \gamma_{3,3} \end{bmatrix} \begin{bmatrix} \tau_{1_{ext}} \\ \tau_{2_{ext}} \\ \tau_{3_{ext}} \end{bmatrix} \tag{4.7}$$

where $\gamma_{i,j}$ denotes the elements of $\mathbf{J}^{-T}$. So, there are eight vertices (2^3) due to the combination of the extreme torque capabilities. Furthermore, the linear

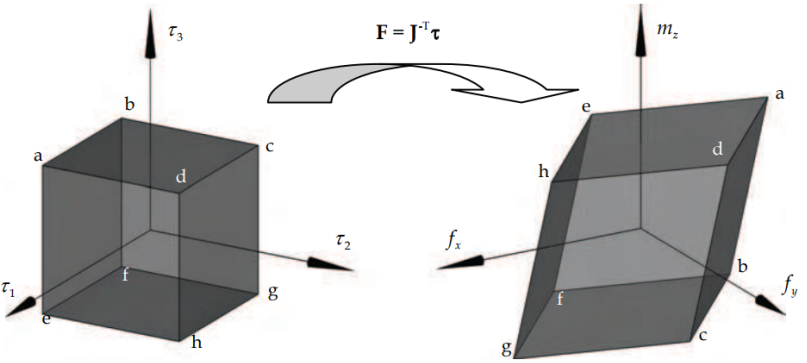

Figure 15: Linear transformation of a parallelepiped to a polytope of a non-redundant parallel manipulator through projection of vertices, edges, and facets. Available at Firmani et al. (2008).

transformation of the torque capabilities of a non-redundant planar parallel manipulator from the torque space to the wrench space is illustrated by Fig. 15. Additionally, the corresponding image of the vertices, edges, and facets between the parallelepiped and the polytope is also shown in Fig. 15.

Finally, Firmani et al. (2008) defines some characteristics of the wrench polytope:

1. Any point outside the polytope is a wrench that cannot be applied or sustained;
2. Any point inside the polytope is achieved with actuators that are not working at their extreme capabilities;
3. Any point on a facet of the polytope has one actuator working at an extreme capability;
4. Any point on an edge of the polytope has two actuators working at their extremes;
5. Any vertex of the polytope has all three actuators working at their extremes.

4.4.4 Redundant manipulators

Additionally, according to Firmani et al. (2008), for redundant manipulators ($n < m$) the number of vertices in the polytope is less than the

vertices of the m-dimensional parallelepiped, i.e., $v_{T_n} < v_{T_m}$. In this case, the polytope vertices are formed with the mapping of some of the vertices of the m-dimensional parallelepiped, i.e.,

$$p_k \subset \mathbf{J}^{-T} v_j \tag{4.8}$$

with $k < j$. Thus, points that do not belong to the vertices of the polytope are internal points in P. Further, all the projected vertices of the m-dimensional parallelepiped in $\mathbb{R}^n$, defined as the potential vertices (p_j) of the polytope are determined as follows:

$$p_j = \mathbf{J}^{-T} v_j \tag{4.9}$$

$$\begin{bmatrix} f_x \\ f_y \\ m_z \end{bmatrix} = \begin{bmatrix} \gamma_{1,1} & \gamma_{1,2} & \cdots & \gamma_{1,m} \\ \gamma_{2,1} & \gamma_{2,2} & \cdots & \gamma_{2,m} \\ \gamma_{3,1} & \gamma_{3,2} & \cdots & \gamma_{3,m} \end{bmatrix} \begin{bmatrix} \tau_{1_{ext}} \\ \tau_{2_{ext}} \\ \vdots \\ \tau_{m_{ext}} \end{bmatrix}. \tag{4.10}$$

Furthermore, the number of external vertices may vary. For instance, a cube's projection on a plane may lead to six external vertices (general projection) or four external vertices (projection normal to a coordinate axis). Thus, the number of vertices of the wrench polytope depends on the pose of the manipulator, which defines the elements of the linear transformation matrix, $\mathbf{J}^{-T}$ (FIRMANI et al., 2008).

Additionally, Fig. 16 illustrates the geometrical interpretation of the internal points of a planar manipulator with redundancy. Thus, the torque capabilities are mapped from $\mathbb{R}^4$ to $\mathbb{R}^3$. Furthermore, the resulting polytope is represented as a wireframe and is formed by the convex hull of the extreme points. As a result, all the subplots of Fig. 16 shows the same polytope with each sub-plot showing regions in which one of the actuator torques is working at its extreme capabilities. In this case, the darker and lighter regions denote the two extremes $t_{i_{min}}$ and $t_{i_{max}}$, respectively. Additionally, the unshaded region represents the space in which the actuator works within its capabilities (FIRMANI et al., 2008).

Hence, while for a nun-redundant manipulator each facet of the m-dimensional parallelepiped corresponded to a facet of the polytope, for a redundant manipulator this projection leads to volumes in the polytope. Also, each edge of the polytope is defined with the projection of three torques set at their extremes; while, each facet is formed with two torques at their extremes. According to Hwang, Lee and Hsia (2000), further actuation would result in more complicated polytopes and the number of internal points will increase

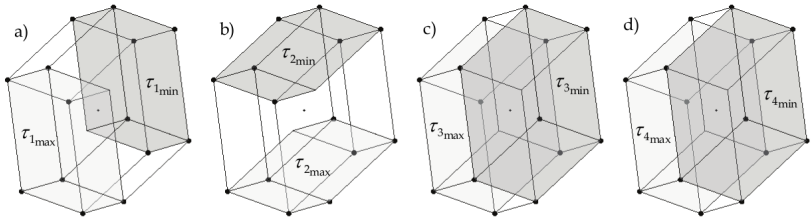

Figure 16: Polytope of a redundant planar parallel manipulator with shaded regions showing torques at extreme capabilities: a) Extremes of τ_1, b) Extremes of τ_2, c) Extremes of τ_3, and d) Extremes of τ_4. Available at Firmani et al. (2008).

exponentially.

Finally, Firmani et al. (2008) also defines some characteristics for the resulting wrench polytope of a redundant manipulator:

1. Any point outside the polytope is a wrench that cannot be applied or sustained;
2. Any point inside the polytope is achieved with actuators that may or may not work at their extreme capabilities;
3. Any point on a facet of the polytope has m-2 actuators working at their extremes;
4. Any point on an edge of the polytope has m-1 actuators working at their extremes;
5. Any vertex of the polytope has all m actuators working at their extremes.

4.5 SCALE FACTOR METHOD

According to Frantz et al. (2015) and Weihmann, Martins and Coelho (2012), the *scale factor method*, presented by Nokleby et al. (2005), consists in the application of a unitary force on the end effector with a desired direction seeking out to define the manipulator joint that is being more loaded in a specific configuration. Thus, this strategy allows to incorporate the saturation limit of the actuators in the problem of *force/moment capability* of robotic manipulators.

In this case, a *unitary screw wrench* ($\$_F$) is used to represent the desired direction of the force in the end effector. Thus, Eq. 4.11 shows the unitary wrench, the force intensity (f_{app}) and the force in the end effector (F_{app}) (NOKLEBY et al., 2005)

$$F_{app} = f_{app}\$_F. \tag{4.11}$$

Further, the wrench in the end effector, F_{app}, can be written dividing the forces portion (f_x,f_y) and the moment(m_z) with $F_{app} = \{f^T; m^T\}$. Thus, since $\$_F$ is unitary and the moment (m_z) is zero, the applied force F_{app} can be represented by:

$$F_{app} = f_{app} \begin{Bmatrix} \cos(\theta) \\ \sin(\theta) \\ 0 \end{Bmatrix}. \tag{4.12}$$

Further, allows to obtain the forces and moments in the manipulator actuators based on the *Jacobian matrix* and the applied force (F_{app})

$$\tau = \mathbf{J}^T F_{app}. \tag{4.13}$$

Furthermore, after the definition of all the torques and forces needed to apply or support an unitary force it is possible to define the scale factor (Φ) of each of the *i* joints' actuators. In this case, the *scale factor* (Φ) of each actuator is the ratio between the actuation limit ($\tau_{i_{max}}$) of the actuator and the torque/force value (τ_i) found for the actuator when a known action is applied defined by (FRANTZ, 2015):

$$\Phi = min \left| \left(\frac{t_{i_{max}}}{t_i} \right) \right|. \tag{4.14}$$

Thus, the *manipulator scale factor* (Φ) is defined as the minimum of the scale factors, indicating the ratio that the known force can be increased without surpass the saturation limit of the most critic actuator. Finally, the

maximum torque/forces, defined as the *force capability* of the manipulator, is defined as the product of the *unitary action* applied initially and the obtained *scale factor*. Thus, he maximum torques/forces (τ) of the actuators can be determined by (FRANTZ, 2015):

$$\tau = \mathbf{J}^T \Phi F_{app}. \tag{4.15}$$

To illustrate, Fig. 17 represents how the initial unitary forces f_x and f_y imply in an unitary *force capability*. Thus, after the application of the *scale factor* the maximum force capability is easily obtained by the factors Φf_x and Φf_y, increasing the force until the saturation limit of each joint actuator.

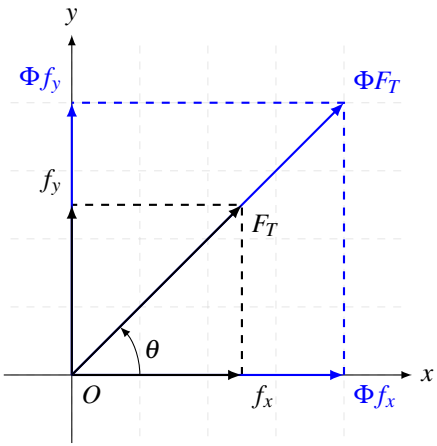

Figure 17: Application of a *scale factor* Φ in the *screw wrench* of the end effector. Available at Frantz (2015).

Further, changing the force (F_{app}) application angle (θ) in a interval [0: 2π] and in the absence of singularities in the Jacobian ($\mathbf{J}$) of Eq. 4.15, the maximum force capability polygon can be obtained, as shown in Fig. 18. This figure shows the force capability of a generic manipulator in the directions x and y when a moment m_z is equal to zero.

Finally, Frantz (2015) proposes Alg. 1 to run the method of Nokleby et al. (2005).

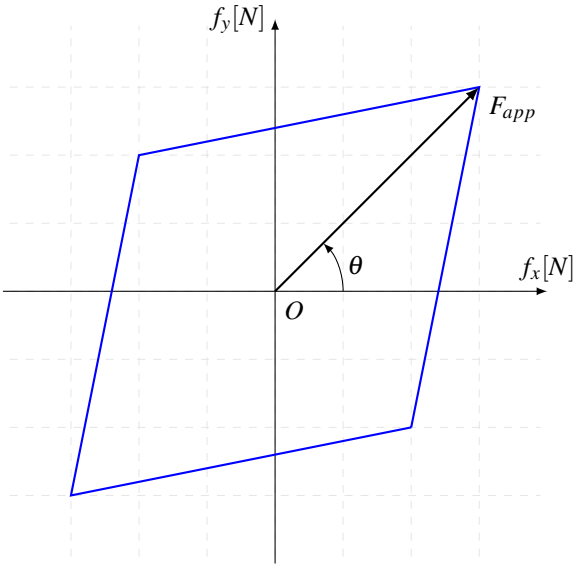

Figure 18: Force capability map of a generic manipulator.

Algorithm 1: Algorithm to calculate the F_{app} by Nokleby et al. (2005). Available at Frantz (2015).

Data: J, τ_{max}, θ and q
Result: F_{app}
Initialization of matrix J;
Initialization of vector of maximum torques τ_{max};
for $0 \leq \theta \leq 2\pi$ **do**
    Definition of the screw wrench vector $\$_F$;
    Calculation of the unitary torques in the actuators τ_i;
    Calculation of the minimum scale factor Φ;
    Calculation of the maximum force F_app;
    Store F_{app};
end

4.6 MOBILE PLATFORM CONSTRAINTS

As presented in Chapter 3, because of its kinematic model, a planar cable driven parallel robot allows the mobile platform to have three dofs in

plane in the same way that a free rigid body would have. Thus, to *exact constraint* the mobile platform the cables actuation must constraint the same three dofs such as the case of Fig. 59b.

For instance, cables that act as actuators could be in two main binary conditions:

- *positive tensioned* by its motors by a tension between a minimum and a maximum value acting as a pure force on the mobile platform

- *sagged* - tensioned by a force that is less that the required minimum to tighten the cables or in absence of tension - and not participating in the definition of the mobile platform position and orientation.

Here, we will analyse how different configurations of cable robots constrain their mobile platform and how it affects its force capability. Furthermore, it is important to define that the force capability of a robot is only defined when its posture is fully defined by its actuators since its end effector must remain statically determined in presence of the external force.

First, the simplest configuration of a cable robot is a planar device with a single cable. Even though this situation seams infeasible even complex devices, such as CRPMs with four cables, will face some situations where just one limb is actuated. In the case of the single cable robot, the actuated limb can act freely in the mobile platform or alongside an external force (f_{ext}). Thus, four combinations are possible. First, the two configurations that are shown in Fig. 19, with only the cable acting(Fig. 19a) and with the external force acting(Fig. 19b) in the same direction of the cable, do not statically define the configuration of the robot and do not belong to its force capability.

Second, Fig. 20a shows a situation where the external force acts oppositely to the single cable force. In this case, if the *constraint lines* are not coincident such as Fig. 20a the mobile platform will remain undetermined. Thus, Fig. 20b is the only that participates in the force capability maps since its *exact constraint* fully describes the position and orientation of the mobile platform. The amount of force that the cable supports is the force capability of the robot in this case.

However, in the situation described by Fig. 20b the *constraint lines* must be exactly coincident. On the contrary, a component such as the f_{ext} in Fig. 21 will appear and lead the mobile platform to instability. In this case, the robot will move until find a position where the external force *action line* becomes coincident with the cable limb line.

Additionally, configurations where two cables are being actuated could lead to situations such as those mentioned before or even define new possibilities. Wherever there is no external force acting on the platform,

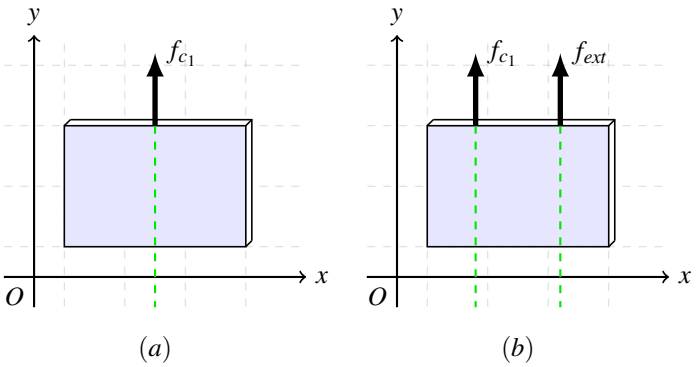

Figure 19: Single limb actuation configurations. (a) without external force and (b) with external force.

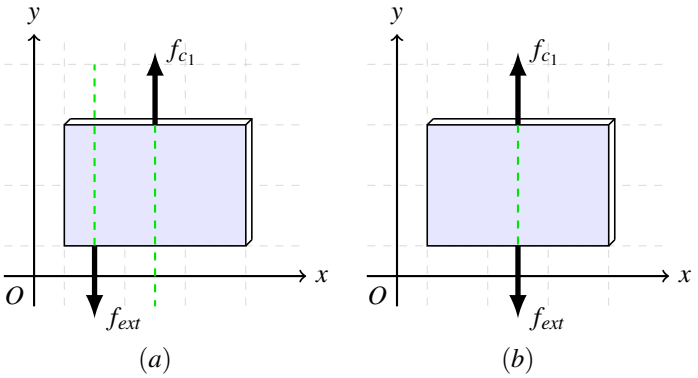

Figure 20: External force acting opposed to the cable force in different action lines(a) and in coincident lines(b).

the possible situations remain the same as the ones with one cable just substituting the external force (f_{ext}) by a cable force (f_{c_2}). In contrast, in situations where an external force acts alongside the cables new possibilities arise. In this case, as proposed by Blanding (1992), it is needed that the external force acts oppositely to the limbs actuations, as showed in Fig. 22, and the cables must have different lines of action, to completely determined the mobile platform posture and force capability.

Further, since the planar motion has only three DoFs, configurations with more than two cables can fully define the mobile platform. However, it

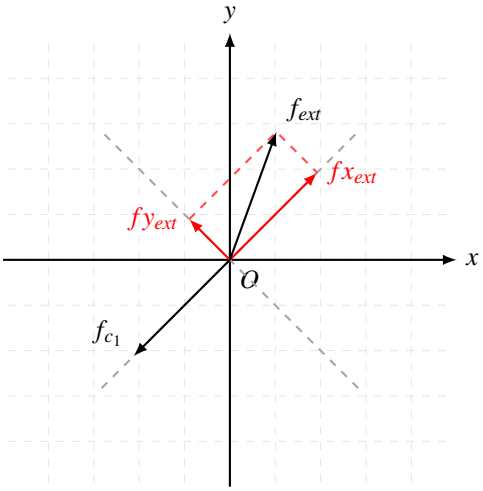

Figure 21: External force components in one cable configuration

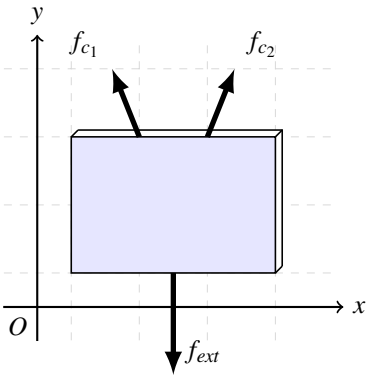

Figure 22: Two cables(f_{c_1} and f_{c_2}) and one external force(f_{ext}) acting in a mobile platform.

is needed that the cables *lines of action* to be different and at least one cable or the external force need to be opposite to some of the cables.

4.7 PROPOSED METHODOLOGY

Force capability methods rely on iterative processes to define the maximum force that a robot is able to exert or support in specific kinematic configurations. Thus, for each type of robot, the required steps in each iteration may be different. In cable robots, its natural reconfigurability requires the robot model to be checked in each iteration. Further, this section will show how the proposed method handles the robot reconfigurability and defines the force capability maps. In this case, the cable robot force capability shows the maximum tension that its cables support according to each external force direction.

The most usual way to define a force capability map is the rotation of a unitary force. In this case, it is possible to define how the robot behaves according to each force direction and also the forces that a robot is able to exert or support in all possible directions given a specified posture. Thus, the proposed method needs to map the cable robots natural reconfigurability. To do so, the cable's unidirectional force behaviour and the fact that only actuated limbs are significant to determine the mobile platform will be taken into consideration using the concepts presented by Blanding (1992) and summarized in Section A.2. Thus, the first step of the proposed method must be the definition of the robots static model according to each force direction.

Cable tensions are only greater than zero when the angle between the external force direction and the cable direction is greater then 90° and smaller that 270°. Thus, this step must define the angles between the external force and the limbs allowing to define which cables are being pulled by the external forces. To do so, each limb tension direction($\vec{c_n}$) and the external force direction ($\vec{f_{ext}}$) were represented as unitary vectors with respect to the same coordinate frame. Further, the following Equation was applied to each limb vector:

$$\vec{c_n} \cdot \vec{f_{ext}} < 0 \tag{4.16}$$

Thus, since the robot model is defined only with tensioned cables, all directions with negative *dot products* are selected. Next, robot configurations that can fully define its posture are selected using the concepts presented by Blanding (1992) and summarized in Section A.2.

Further, it is also needed to define the solving techniques that will be used for each configuration. Moreover, the chosen techniques are based in the robot static model and in the solutions that are obtained when a unitary force is applied. Thus, some solving methods, presented here, were gathered in a way that could allow the proposed method to solve all the possible robots

configurations and finally obtain the whole force capability map. In this case, each of the solving methods are summarized here according the number of actuated cables:

- First, in a **single cable** configuration the force capability is only defined as a line of action opposed to the cable force. All other external force directions are not able to define the posture of the cable robot. In this case, the force capability is defined only by the cable maximum force with no solving method needed;

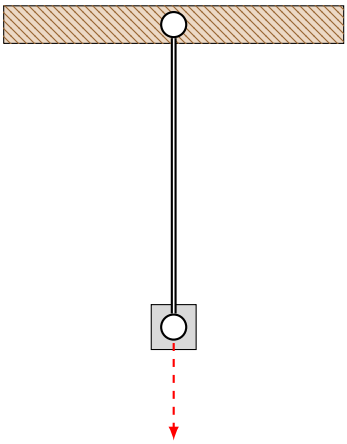

Figure 23: Force capability of a single cable.

- Second, the *lines of action* of configurations with **two cables** are analysed. If they are coincident, the force capability is equivalent to configurations with a single cable with the force of both actuators added. In other cases, the angle between the lines of action will define a range where the external force can be applied, according to the principle of exact constraint. Thus, Fig. 24 shows the range where an external force can be sustained by two cables. In this case, the shape of the polytope will be defined by the actuator's force. In this case, for each external force direction the **modified scale factor** will be applied as the solving method.

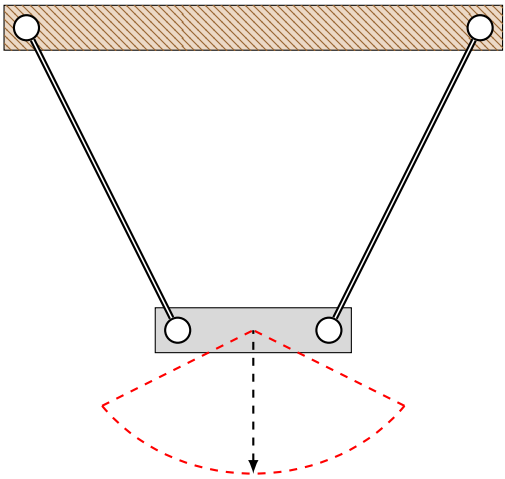

Figure 24: Force capability range of two cables.

- Third, **optimization methods** are used to define the force capability for configurations with **more than two cables**. If the **lines of action** are coincident, the range will be restricted to a single line. If only two **lines of action** are non-coincident, the range is defined in the same way as configurations with **two cables**. For three of more non-coincident cables, the external force possible range will be defined by the maximum angle between two of the actuated cables.

Finally, after the definition of the solving method and the robot model, the force capability in the desired direction is obtained. Then, the iterative method can move to the next desired direction. The proposed methodology is summarized in the Fig. 25 and in the Algorithm 2.

Algorithm 2: Proposed methodology to define the map of force capability of cable robots.

Data: τ_{max} and $[A_n]$
Result: F_{app}
for $0 \leq \theta \leq 2\pi$ **do**
    Definition of the number of actuated cables (dot product) n_c;
    Definition of the matrix J by the number of actuated cables n_c;
    if $n_c = 1$ *and the dot product = -1* **then**
        F_{app} is equal to the maximum cable force;
    else if $n_c = 2$ **then**
        Define F_{app} by the *scale factor* method;
    else if $n_c > 2$ **then**
        Define F_{app} by a *constrained optimization* method;
    else
        $F_{app} = 0$;
    end
    Store F_{app};
end

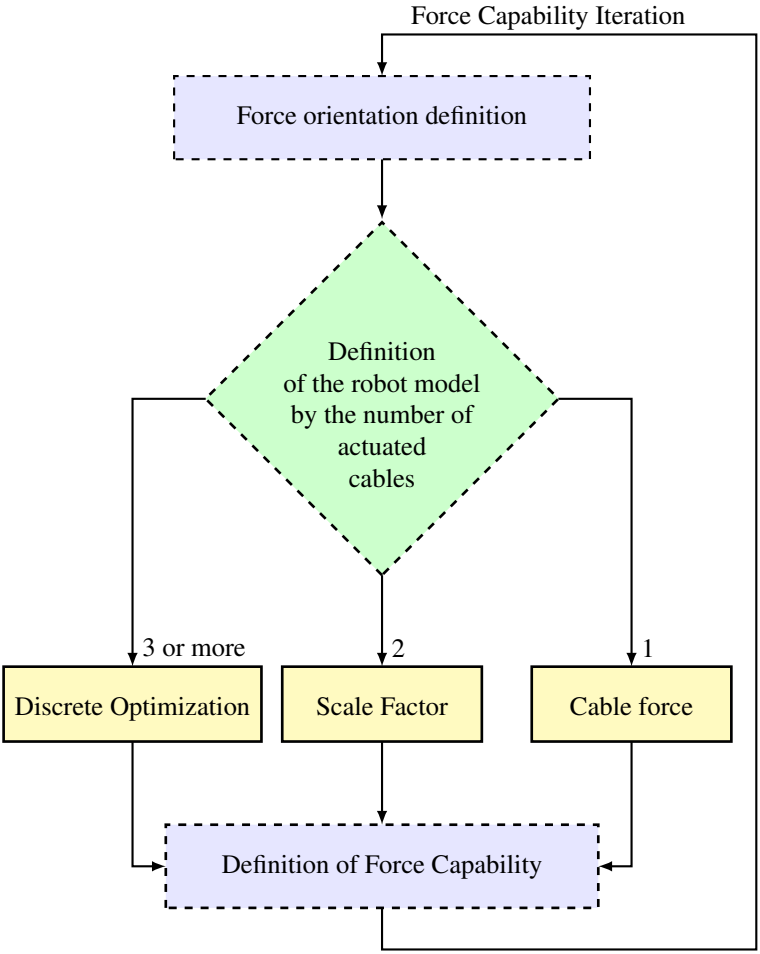

Figure 25: Summary of the proposed Method

4.8 CASE STUDIES

To illustrate concepts that were shown in previous sections case studies will be exhibited. First, the static model of a planar CDPR(Fig. 26) presented in the Chapter 3 will be applied to solve the force capability of a robot with two cables. In this case, the robot range of action will be analysed before the definition of the force capability aiming to reduce the number of iterations needed to fully define the map.

Further, configurations with three and four cables will also be analysed. Thus, the robot behaviour will be better understood and the steps of the proposed method verified.

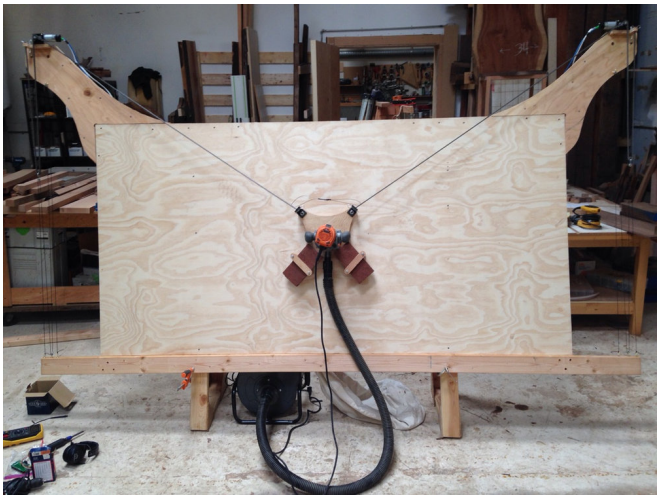

Figure 26: Planar Cable Driven Robot for cutting wood - Maslow CNC. Available at Maslow (2018).

4.8.1 Case 1: Planar CDPR with two cables

In the first case study, the robot design is defined by two cables (Fig. 27), actuated by motors that are able to generate 1 N of force in each of the robot legs. In this case, O_m defines the central point of the mobile platform and is horizontally centred with the base. Since in this position the robot is symmetric the maximum force capability happens when the external force is acting perpendicularly to the mobile platform and opposed to the cable forces. The mass and strength of the cable were ignored.

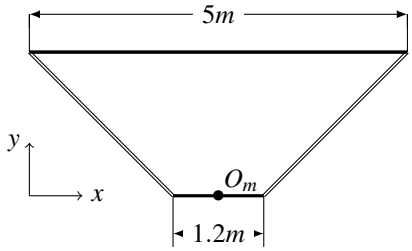

Figure 27: Robot configuration of a two cables CDPR.

Table 3: Dimensions of the Planar CDPR with two cables.

Component	Dimension
Robot Height	1.9 m
Mobile Platform Width	1.2 m
Base Width	5 m

Following the steps proposed in our methodology, the first definition is the robot static model (Chapter 3). Further, the force capability iterative process can starts. However, since the map feasible angle is significantly reduced in two cables configurations, a preprocessing can be done to reduce the number of iterations.

The preprocessing first step is verify positions where the cables are being actuated. Thus, since the tension will be greater than zero only when the angle between the external force and each cable is greater than 90° and less than 270° two perpendicular lines to each cable can be used to define the force capability feasible angle (θ_{cap}), Fig. 28. Finally, the definition of 2-RPR robot force capability can be constrained to external force angles that lay inside this feasible space.

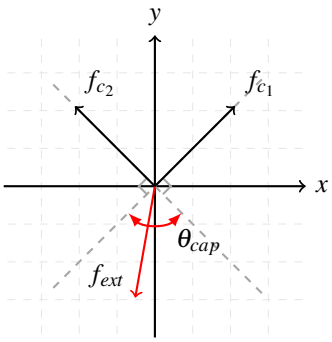

Figure 28: Force capability angle (θ_{cap}) in a two cable configuration.

Second, a solving method may be applied to find the force capability within the range defined by θ_{cap}. In this case, for each desired angle inside θ_{cap} the *scale factor* method must be applied as presented by Weihmann (2011), Frantz (2015), Mejia (2016) and Nokleby et al. (2005).

Finally, after all the steps of the iterative process a *force capability map* is obtained (Fig. 29). In this case, the desired configuration had only two cables. However, the *scale factor method* can also be used in more complex robots in situations where just two cables are being actuated.

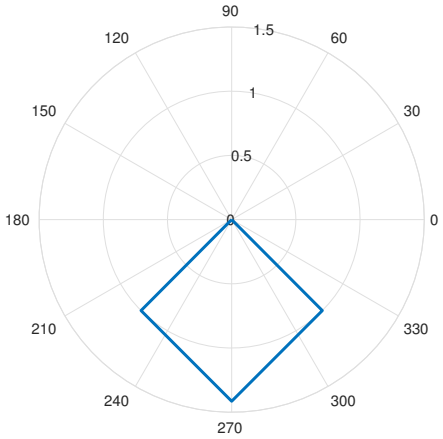

Figure 29: Force capability polar map of a two cables CDPR .

4.8.2 Case 2: Planar CDPR with three cables

Expanding the analysis of planar CDPRs, a configuration with three cables is defined in Fig. 30. In this case, the base and the mobile platform are triangular with dimensions ($5m$,$5m$) and ($1.25m, 1.25m$), respectively. Further, each cable is able to exert a tension of $1N$. The center of mass of the mobile platform (O_m) defines its position. In this section, the *force capability map* is defined in two O_m positions.

Further, since in this configuration it is impossible for an external force to act on three cables simultaneously just the scale factor method and the single cable force is enough to define the *force capability map*. Thus, a static model and a *Jacobian matrix* must be defined for each pair of cables and the iterative process must select a static model for each external force direction.

Finally, the *force capability map* is defined as the composition of the maps of each two cables configuration. Furthermore, a configuration where three cables acts simultaneously will be also analysed.

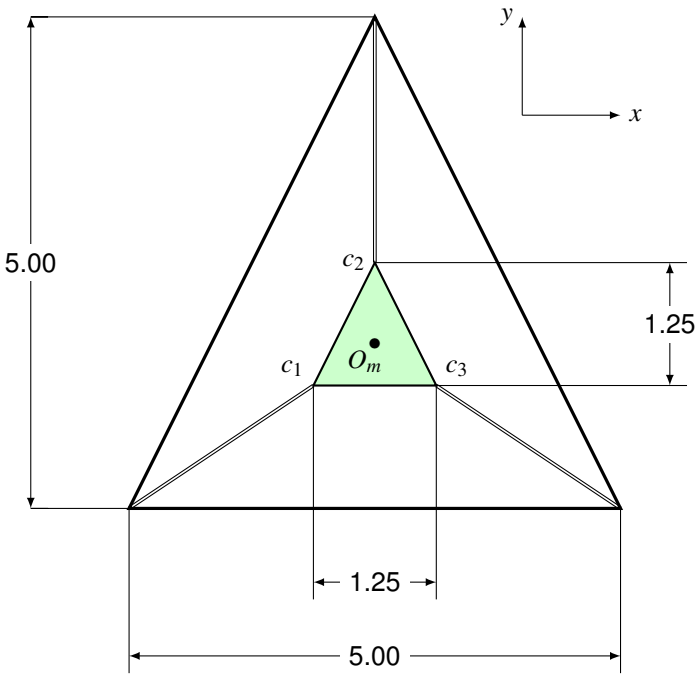

Figure 30: Planar CDPR with three cables.

First, a configuration where the center of mobile platform (O_m) is positioned in the center of the base is selected. In this case, the angles between each pair of actuated cables are equal. Thus, since the force capability of each of the cables are all the same the *force capability map* must be symmetric.

Fig. 31 shows the *force capability map*, in a polar plot, of this planar robot configuration. In this case, since only two cables are being actuated, the *Jacobian matrix* is obtained only by the static model available in Chapter 3.

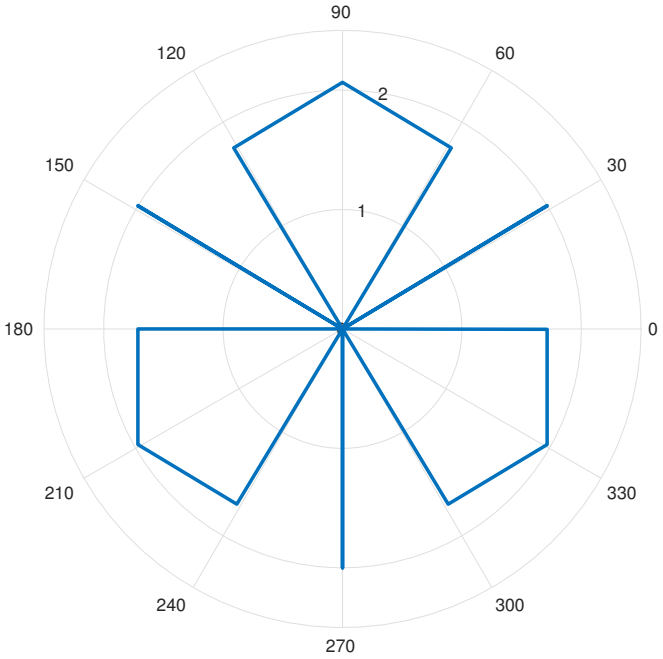

Figure 31: Force Capability of a 3-RPR with O_m centred - Polar Plot.

Further, Fig. 32 shows how each cable is being actuated alongside the range of external force angle.It is important to denote that actions outside the range of the *force capability map* will lead to undesired motions in the end-effector.

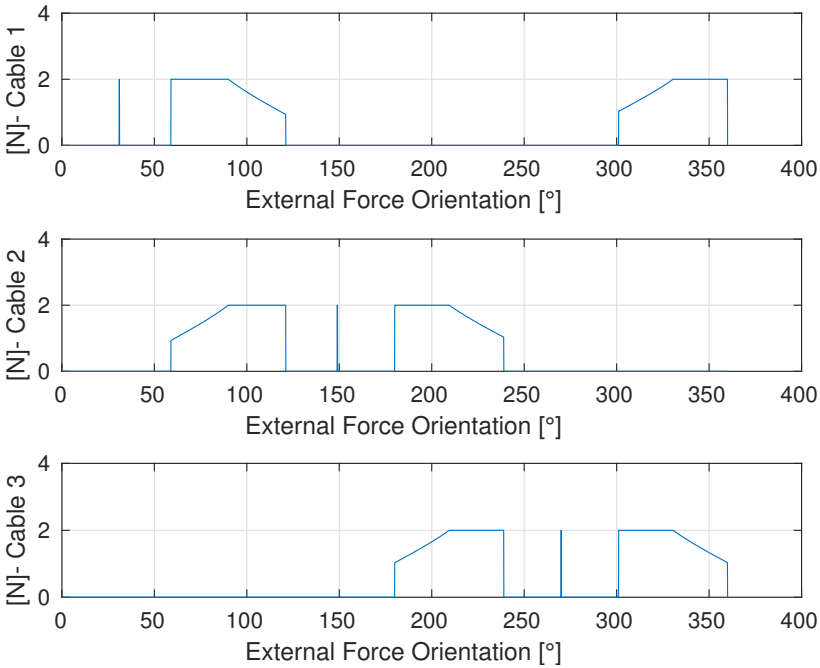

Figure 32: Force Capability of a 3-RPR with O_m centred - Cable Forces Plots (N per degree) for each cable.

Furthermore, Fig. 33 shows the *force capability map* for the planar CDPR of Fig. 30 but with O_m moved from the center of the base to the position $(2,2)$. In this case, the map symmetry of Fig. 31 is not maintained and the force capability in north and south-west directions decreases, while, in the south-east direction, it increases.

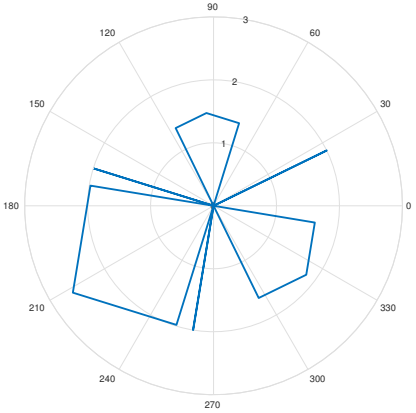

Figure 33: Force Capability of a 3-RPR - O_m in $(2,2)$ - Polar Plot.

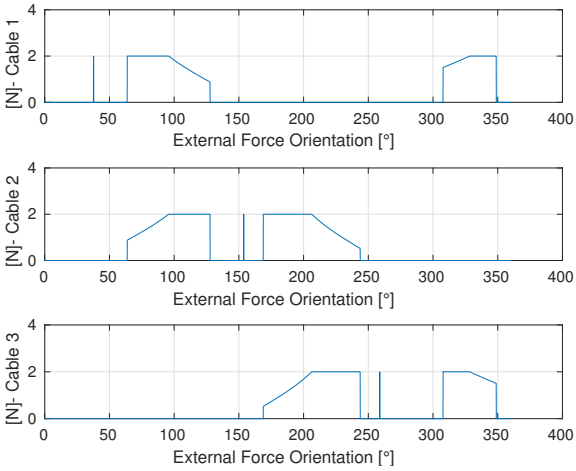

Figure 34: Force Capability of a 3-RPR - O_m in $(2,2)$ - Cable Forces Plots (N per degree) for each cable.

Additionally, a CDPR with three acting cables (Fig. 35) is analysed by the proposed method. In this case, the *constrained optimization* was the solving method used in the external forces feasible angle. Thus, Fig. 36 shows the Cartesian plot of this configuration *force capability map* considering three cables that are able to exert 1 N each.

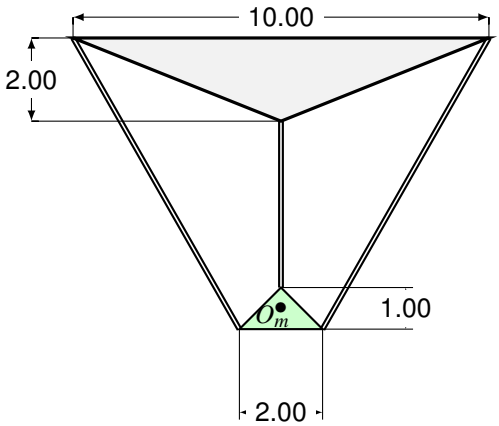

Figure 35: Configuration of a 3-RPR - Cartesian Plot.

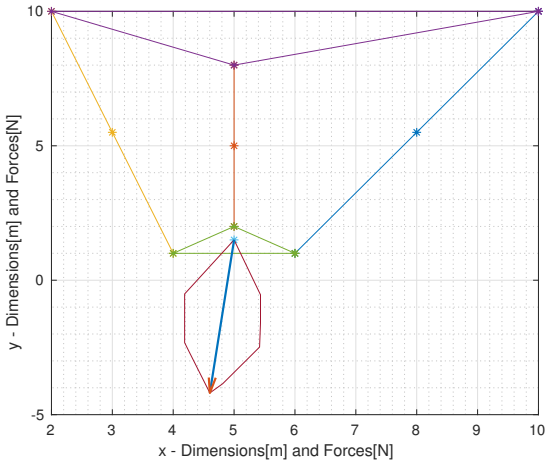

Figure 36: Force Capability and Configuration of a 3-RPR - Cartesian Plot.

4.8.3 Case 3: Planar CDPR with four cables

Finally, a planar CDPR with four cables is analysed. In this case, eight *Jacobian matrices* must be defined, being four for each combination of three subsequent cables and four combinations of pairs of subsequent cables. Thus, for two cables configurations the combinations are: $c_1 - c_2$, $c_2 - c_3$, $c_3 - c_4$ and $c_4 - c_1$. Among configurations with three cables, $c_1 - c_2 - c_3$, $c_2 - c_3 - c_4$, $c_3 - c_4 - c_1$ and $c_4 - c_1 - c_2$ selected.

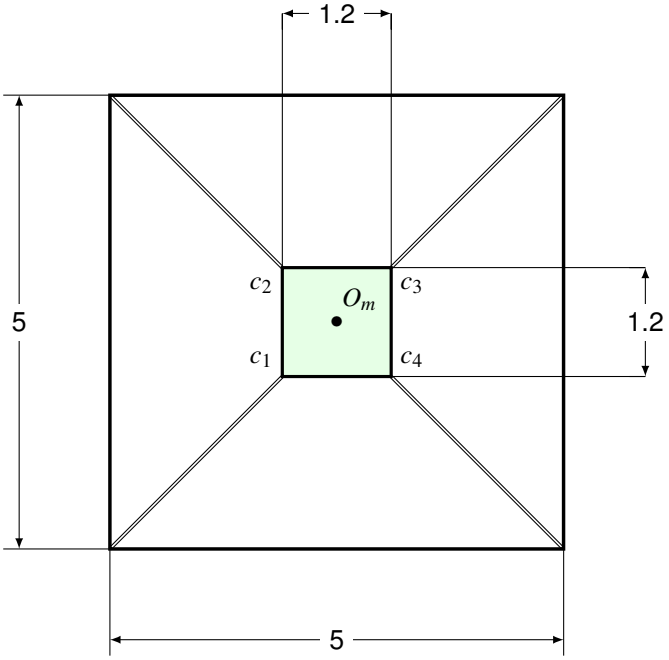

Figure 37: Planar CDPR with four cables.

Again, the force capability map of this planar CDPR will change according to the position of the mobile platform center (O_m). In this case, if the mobile platform is positioned in the center of the base (Fig. 38), the force capability map can be fully defined by the scale factor method, because in this case, there is no external force angle where more than two cables are being actuated.

Further, Fig. 39 shows how each cable is being actuated according to changes in the external force angle.

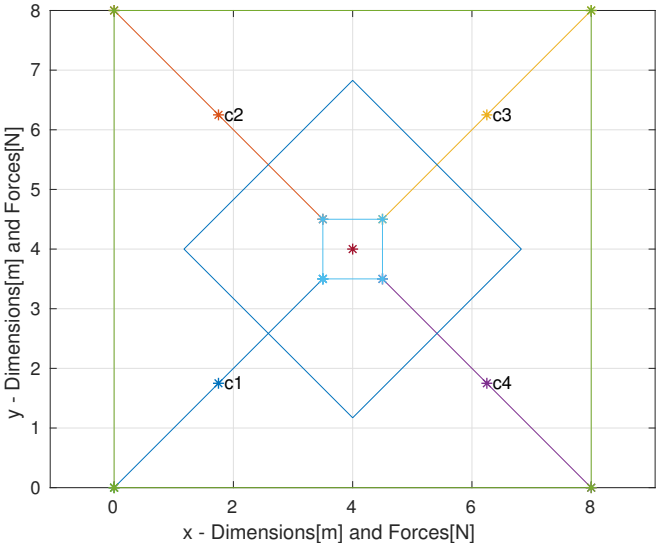

Figure 38: Force Capability of a 4-RPR - Cartesian Plot.

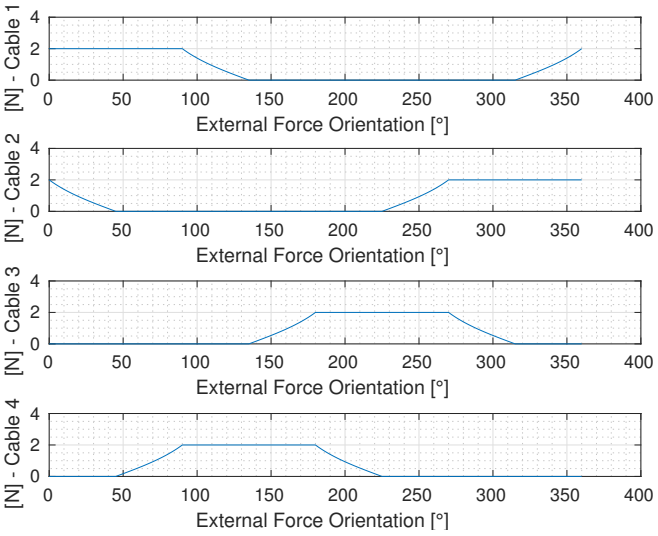

Figure 39: Force Capability of a 4-RPR - Cable Forces Plot.

Finally, moving O_m in any direction outside the center of the base it is possible to fully apply the proposed method to analyse the force capability of a CDPR. Thus, Fig. 40 shows a *force capability map* of a CDPR obtained by the proposed method. Further, Fig. 42 shows how the forces in the robot cables changes according to the external force angle. In this case, the angular **gaps** (Fig. 41) inside the force capability map are due to directions where only one cable is acting and the external force is not able to fully define the platform position and orientation.

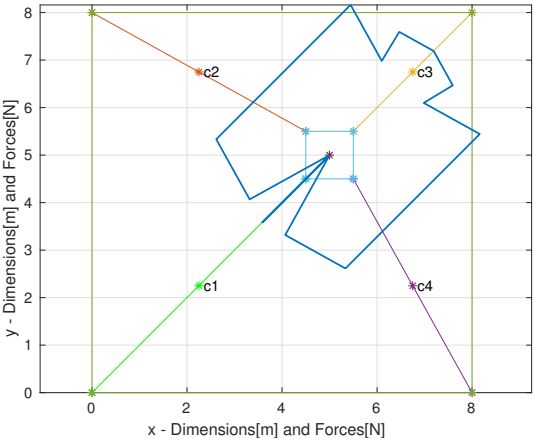

Figure 40: Force Capability of a 4-RPR - Proposed Method - Cartesian Plot.

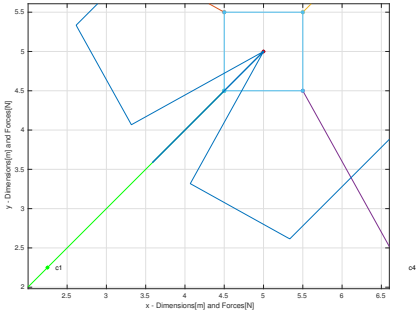

Figure 41: Zoom in the Force Capability of a 4-RPR - Proposed Method - Cartesian Plot.

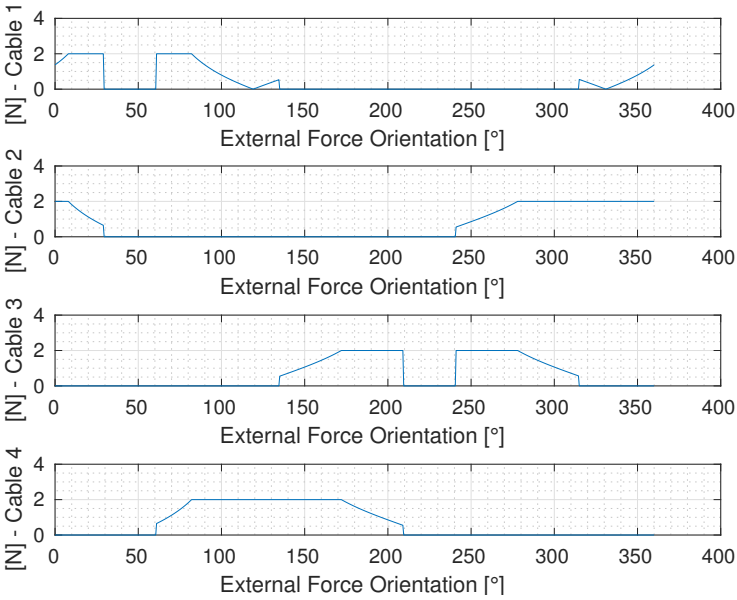

Figure 42: Force Capability of a 4-RPR - Proposed Method - Cable Forces.

4.9 CONCLUSIONS

Force capability stands as one of the main parameters of robot performance. With this indicator, a trajectory or task can optimized and a better suited robot can be picked. Regarding cable robots, the unidirectional force behavior and the natural reconfigurability makes the definition of the force capability more complex and important. Since forces in undesired directions are able to remove the robot from the desired position. However, besides the importance of force capability maps, the amount of computational power and time required makes the use of this performance parameter unusual. The proposed method reduces significantly the time and complexity of the problem and could be applied to increase the use of this parameter.

5 DISCUSSION ON CABLE ROBOTS FORCE CAPABILITY

According to Abdelaziz et al. (2017), the available force set that a four cables configuration (Fig. 43) is able to exert has the octagon of Fig. 44.

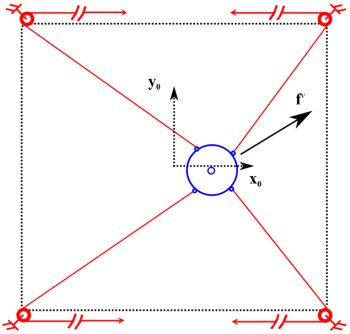

Figure 43: 4 cables CDPR evaluated by Abdelaziz et al. (2017). Available at Abdelaziz et al. (2017)

In this case, according to Abdelaziz et al. (2017), the *force capability map*(Fig. 44) in this configuration and position is defined for all external forces directions.

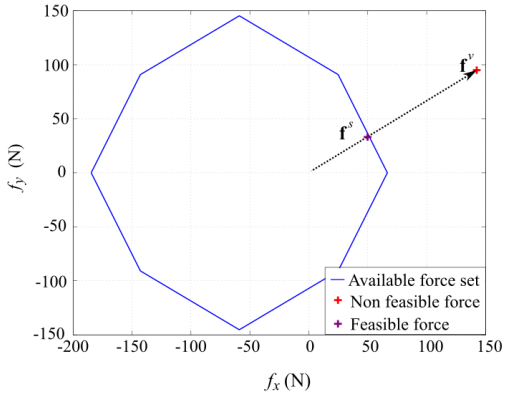

Figure 44: Available Force Set of a 4 cables CDPR. Available at Abdelaziz et al. (2017)

However, according to the principles of *exact constraints*, presented by Blanding (1992), some external force directions would lead to an under-constrained mobile platform and thus should not be presented in the force capability map of this configuration. Thus, a *constrained optimization* method was applied to try to simulate Abdelaziz et al. (2017) aiming to achieve the same results.

In this case, the constraint about the number of actuated cables was removed from the analysis. Fig. 45 shows the *force capability map* that was obtained while Fig. 46 shows the force distribution in the robot actuators. As expected, some external forces angles leads to situations where just one cable is acting which does not obey to the exact constraint principle.

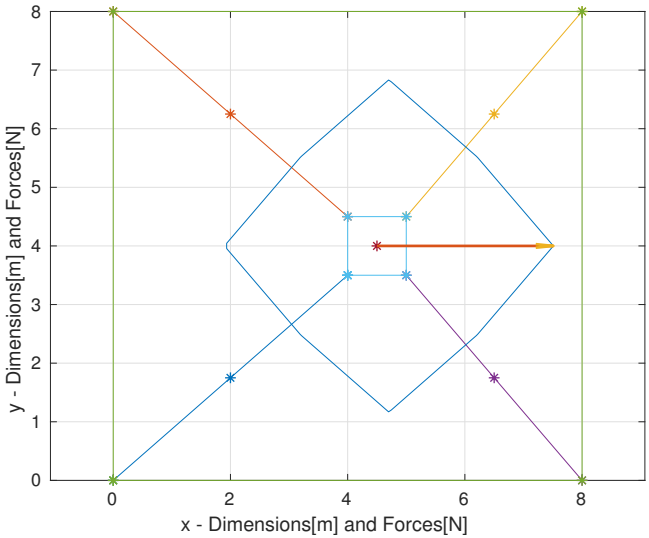

Figure 45: Force Capability Map by Constrained Optimization - O_m at (4,4.5)

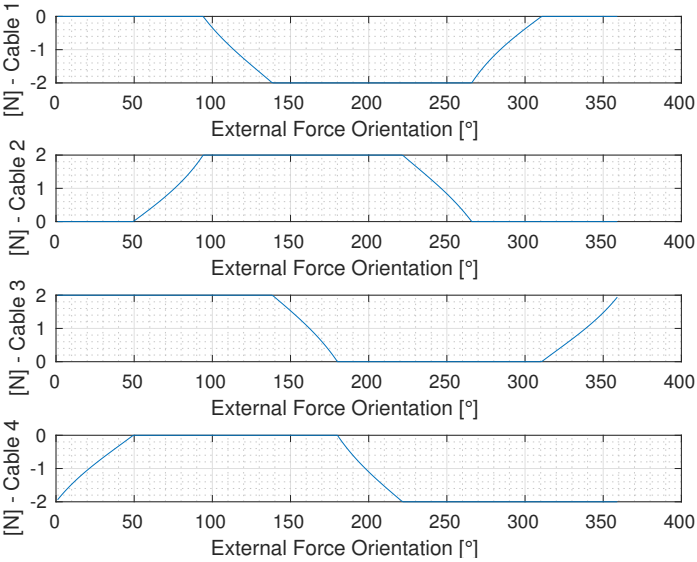

Figure 46: Cable Forces according to the external force angle - O_m at (4,4.5)

Further, the proposed method was applied to contrast with the results obtained by Abdelaziz et al. (2017). In this case, Fig. 47 shows that there are some external force angles that cannot be sustained(such as the discontinuities near the left cables) in this position contrasting to the solution presented by Abdelaziz et al. (2017). Finally, Fig. 48 shows that with our proposed method the principle of *exact constraint* is obeyed.

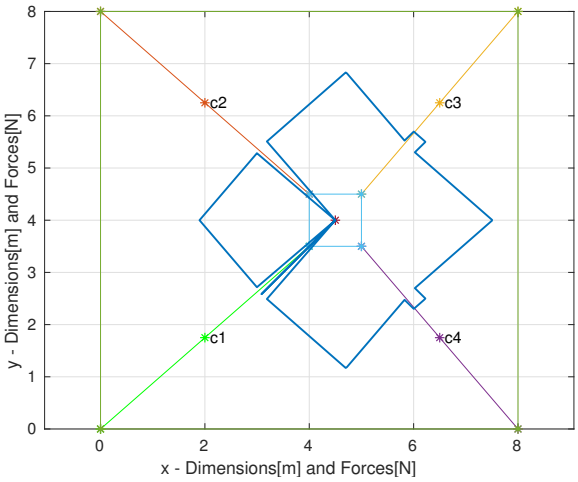

Figure 47: Force Capability Map by the proposed Method - O_m at (4,4.5)

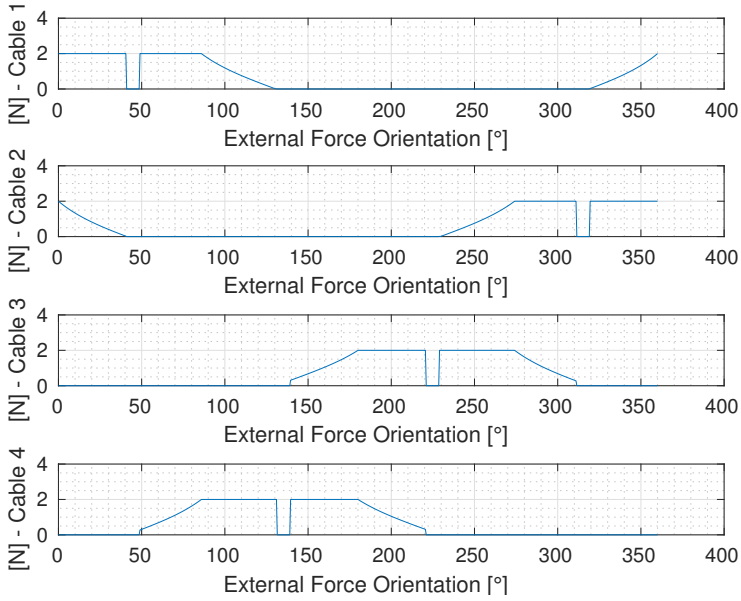

Figure 48: Cable Forces according to the external force angle - O_m at (4,4.5)

5.1 CONCLUSIONS

The works of Abdelaziz et al. (2017) are one of the most recent publications in the field of cable robots about force capability. However, according to Blanding (1992) principles, some of its maps are infeasible by conventional cable robots. This chapter presented how he was able to obtain the maps and how the maps should be defined. In this case, the proposed method also presents a more conservative approach since its guarantee the platform pose for all feasible directions. Finally, there was a gain of computational performance as well since most of the obtained map was done through the **scale factor method**, a much faster approach when compared to optimization methods.

6 CABLE ROBOTS WORKSPACE

According to Gosselin (2014) there are many ways to define the workspace of a robot manipulator. First, Sciavicco and Siciliano (2000) define the *reachable workspace* as a volume in space where the geometrical center of the mobile platform (O_m) can act, whereas the *dextrous workspace* is defined as a subset of reachable positions based on pre-determined end effector orientations. Bruckmann et al. (2008) define the workspace as one of the main performance characteristic of robots and as an open issue in the study of cable robots.

Moreover, the workspace definition is directly related to the robot topology, mainly by their links size and actuators capabilities. Further, in the study of cable robots there are several definitions of the workspace, among them the most significant are: *dynamic workspace*, *static workspace*, *force closure workspace*, *wrench closure workspace - WCW*, *wrench-feasible workspace - WFW*, *force-closure workspace - FCW* and *interference free workspace*.

Barrette and Gosselin (2005) define the *dynamic workspace* as a set of all configurations and dynamic conditions where the cables tensions are positive. Pusey et al. (2004) analyse the *static workspace* using the static equilibrium of forces and moments at the robot end effector taking in consideration only gravity as external force. In this case, the volume of the *static workspace* is defined as the set of points where the center of mobile platform can reach with all its cables tensioned. However, Barrette and Gosselin (2005) define the *static workspace* as the *dinamic workspace* with all accelerations null.

Further, Lau, Oetomo and Halgamuge (2011) and Gouttefarde and Gosselin (2006) address the *wrench-closure workspace - WCW* as the set of end effector postures where the manipulator is able to sustain a specific set of external forces and moments, without restraining the forces that each cable is able to perform.

Furthermore, the *wrench-feasible workspace - WFW* is defined as a subset of *WCW* where the maximum forces in each cable is imposed as restrictions. In this case, the *WFW* is define as the set of postures where the dynamic system can be satisfied by positive forces acting on the robot cables for a specific set of external forces, moments, velocities and accelerations satisfying a set of restrictions in the robot cables (GOUTTEFARDE; MERLET; DANEY, 2007). However, Bosscher (2004) defines *WFW* as set of postures where the manipulator is able to exert a set of forces and moments (*wrenches*). In this case, this region constitutes the workspace that is used by the robot for

an specific application.

Also, the *force-closure workspace - FCW* is defined by (PHAM et al., 2006) as the set of postures where the equilibrium of forces is satisfied. According to Diao and Ma (2007), a CDPR finds a condition of forces equilibrium for a specified posture if, and only if, any set of external forces and moments applied to the mobile platform can be sustained by a set of positive cable forces. For Lau, Oetomo and Halgamuge (2011). the set define by the *FCW* is the same of *WCW*.

Additionally, Lau, Oetomo and Halgamuge (2011) analyses the concept of *interference free workspace*, which is related to the cable collisions within themselves or with the environment. Thus, this concept analyses geometrical characteristics such as the cable positions and the environment leading to collisions free paths.

6.1 PROPOSED METHOD

The proposed method for *force capability* allows to define the set of *wrenches* that a robot is able to apply or support in a predefined position. However, sometimes, the robot has to apply or support a set of *wrenches* alongside a *trajectory* or within a *workspace*.

Thus, our proposed method was expanded to deal with changes in the mobile platform position allowing to define a wrench-feasible trajectory and workspace (WFW). In this case, the trajectory and workspace will be discretized and the robot force capability will be discretely solved for every point. Further, this approach could help to understand more about the robot behaviour and show information such as the weight that a robot is able to carry during a movement or to help planning a trajectory to reduce the power consumption of the robot.

The first step of the proposed method is to define the set of *wrenches* directions that the robot will have to apply or support. Second, the trajectory or the workspace range may be defined and discretized. Third, the *force capability* is defined for the desired wrench direction and for each of the O_m discretized points. Finally, a map is defined with the maximum force that the robot is able to support or apply in the predetermined range.

Further, the computational steps to define these maps are summarized in algorithm 3. In this case, $\{\tau_{max}\}$ represents a vector of maximum forces for the robot cables, $\{\theta\}$ is the vector of desired directions of the external wrench and $[D_{O_m}]$ is the matrix of desired positions for the robot end effector. For each point in $[D_{O_m}]$, a maximum F_{app} is defined within the range determined by $\{\theta\}$.

Algorithm 3: Proposed methodology to define the wrench-feasible workspace and trajectory of cable robots.

Data: $\{\tau_{max}\}$, $\{\theta\}$ and $[D_{O_m}]$
Result: $[F_{app}]$
foreach $[D_{O_m}]$ **do**
  Definition of the action matrix $[A_n]$;
  foreach $\{\theta\}$ **do**
    Definition of the number of actuated cables (dot product) n_c;
    Definition of the matrix J by the number of actuated cables n_c;
    if $n_c = 1$ *and the dot product = -1* **then**
      F_{app} is equal to the maximum cable force;
    else if $n_c = 2$ **then**
      Define F_{app} by the *scale factor* method;
    else if $n_c > 2$ **then**
      Define F_{app} by a *constrained optimization* method;
    else
      $F_{app} = 0$;
    end
    Store F_{app};
  end
end

Besides, the planar robots *wrench-feasible workspace (WFW)* or *trajectory (WFT)* can be represented in a cartesian map with the **force capability** defined by colors, if there is only one *desired direction* or the focus is just the maximum or minimum force within that range. Furthermore, configurations with a greater number of desired directions will need more complex representations.

Finally, sections 6.1.1 and 6.1.2 will show some examples about the definition of the WFW and the WFT, respectively. In this case, just a single θ is used to define the maps to allow better representations of the maps.

6.1.1 Wrench-Feasible Trajectory

Robots, such as palletizers, must carry loads, such as boxes, horizontally to the soil within all its workspace. In this case, since the robot *force capability* changes according to its position the maximum load that the robot

is able to carry during all the trajectory must be defined by the position that has the minimum force capability. Thus, it is guaranteed that the robot will handle any load within this range in that trajectory without surpass the *wrench capability* of its actuators.

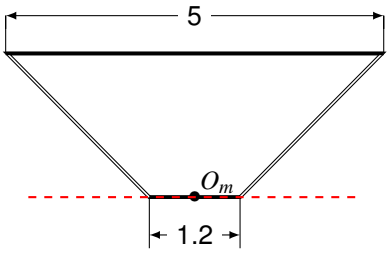

Figure 49: Cable Robot Configuration and Desired Trajectory

Further, Fig. 49 shows a planar CDPR with two cables and a desired horizontal trajectory (red dashed line). In this case, since the objective is to carry loads parallel to the soil the *force capability* is defined vertically in the same direction as the gravity vector. Futhermore, Fig. 50 shows the *force capability* alongside a *wrench-feasible trajectory* of this cable robot. In this case, the extremes horizontal positions will define the maximum load that the robot is able to carry.

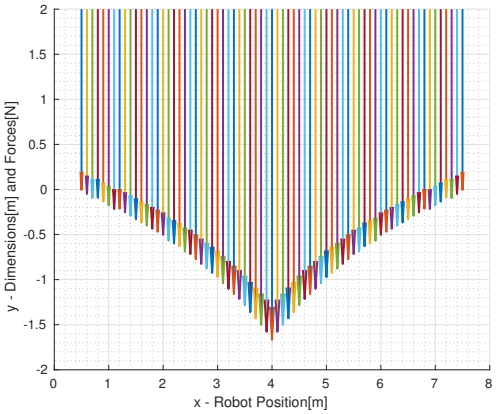

Figure 50: Vertical Force Capability Trajectory.

6.1.2 Wrench-Feasible Workspace

Further, a *wrench-feasible workspace* represented in Fig. 49. In this case, the $[D_{O_m}]$ matrix was discretized in X and Y and the θ angle defined in the same direction as gravity such as the *wrench-feasible trajectory*. Furthermore, Fig. 51 shows the *wrench-feasible workspace* for vertical forces of the two cables CDPR. Thus, it is possible to observe that it is better to define trajectories and carry loads far from the base and close to the middle of the robot.

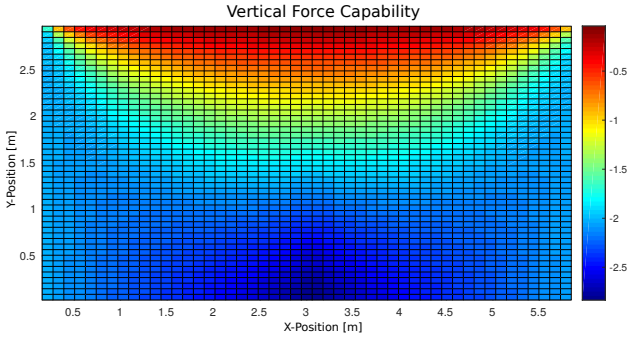

Figure 51: Wrench-Feasible Workspace.

6.2 CONCLUSIONS

The main operational aspect of a robot is to move its end-effector according to a required task. In this case, as presented before, the task could require the end-effector to support or apply an specific wrench alongside an trajectory or within a defined space. Thus, the definition of a single force capability map is not enough to completely analyze the robot. In this case, the wrench-feasible workspace provides a much wider analyses of the system and is significantly improved by the method proposed by this project. The main reason for this improvement is the time reduction provided by pre-processing using the concept of exact constraint.

7 CONCLUSIONS

According to Gosselin (2014), the full potential of cable-driven parallel mechanisms has not yet been exploited. He claims that future applications in several areas are to be expected which, in some cases, have the potential to rewrite the rules of robotic manipulation. However, the growth of this area is significantly connected to the results obtained through its research on laboratories.

Thus, the main goal of this project is to provide useful information regarding this equipment and contribute to its implementation. In this case, this goal was achieved through a novel method that is able to build force capability and wrench-feasible workspace maps.

Many performance parameters are important to choose and optimize robots. In this project, the force capability was selected as the main indicator mainly because one of the main aspects of cable robots is its ability to easily handle large workspaces and high payloads and thus it is crucial to understand how the payload will be handled inside a task space or during a trajectory. It is also important to understand how to optimize tasks and trajectories to take the best out of cable robots.

The main contribution of this project was the development of an optimized method to define CDPRs' force capability, based on mechanism theory. In this case, the optimization aims to reduce the computation time needed to fully define a force capability map. To do so, some well understood concepts, such as the Davies' Method, the exact constraint, the scale factor and constrained optimization were applied alongside a smart switch algorithm.

The first accomplished task was the definition of the robot mathematical model. To do so, each cable was modelled as a RPR structure and the tightening conditions treated as a natural reconfigurability. In this case, the Davies' method is applied to solve the robot model while loosen cables are removed from the robot model. Moreover, the robot mobile platform was analysed as a free body that should be exact constrained by the cables and external forces to fully define its pose.

Two solving methods were mainly applied in this project, the modified scale factor and the constrained optimization. In the first, solutions are obtained without iteration but its application is restricted only for planar systems with two cables. Additionally, configurations with more actuated cables requires iterative methods such as the constrained optimization. Finally, the main aspect of this project was smartly switch through this approaches and the robot models optimizing the definition of force capability

and wrench feasible maps.

The proposed method was presented through some case studies and a discussion. The main goal of the discussion was to reveal that even with a more conservative approach our method could lead to better and faster results and guarantee the robot pose through all the force capability map positions.

Finally, the smart switch approach, one of the main contributions of this work, could be applied for any kind of reconfigurable system allowing to improve the application possibilities of the Davies' Method.

7.1 PUBLICATIONS

Alongside the research done during this work, some developments about the creative design of mechanisms were also done. This resulted in the following papers:

- *An innovative methodology for toggle clamping device design* (COSTA, M. V. O.; MURAI, E. H. ; ROSA, F. S. ; MARTINS, D.). In: 24th ABCM International Congress of Mechanical Engineering, 2017, Curitiba - PR. Anais do 24th ABCM International Congress of Mechanical Engineering, 2017.

- *Review and classification of workpiece toggle clamping devices* (COSTA, M. V. O.; MURAI, E. H. ; ROSA, F. S. ; MARTINS, D.). In: 6th International Symposium on Multibody Systems and Mechatronics, 2017, Florianopolis. Multibody Mechatronic Systems: Proceedings of the MuSMe Conference, 2017.

- *State of the art of cable driven robot for transfer of bedridden patients* (FRANTZ, J. C. ; MURARO, T. ; MARTINS, D. ; ROSA, F. S. ; COSTA, M. V. O. ; LUCA, M. R.). In: I Congresso Brasileiro de Pesquisa & Desenvolvimento em Tecnologia, 2016, Curitiba. I Congresso Brasileiro de Pesquisa & Desenvolvimento em Tecnologia, 2016

7.2 SUGGESTIONS FOR FUTURE WORK

One of the main aspects of the Davies' Method application is the possibility to expand the proposed method to any mechanism. Thus, the results obtained through this research led to the following suggestions for future work:

- To define the force capability of hybrid systems using cables and rigid links such as exoskeletons.
- To define or propose the force capability of cooperative systems (Fig. 52) with cables and conventional robots.

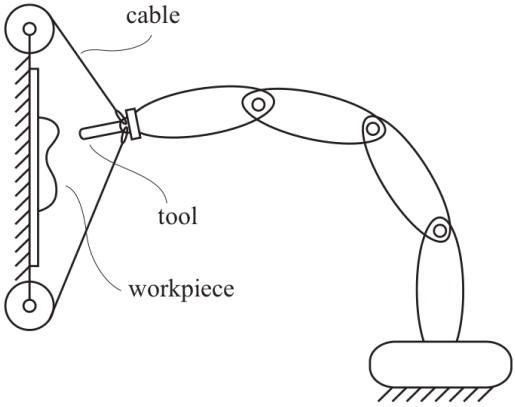

Figure 52: Cooperative System with Cable and Serial Robots

- To expand the proposed method for spatial cable driven parallel robots.
- To define optimum trajectories based on the wrench feasible workspace.
- To define the velocity capability, the power capability and the efficiency of robot models and tasks.
- To define a force controller for cable driven parallel robots.

BIBLIOGRAPHY

ABDELAZIZ, S.; BARBé, L.; RENAUD, P.; MATHELIN, M. de; BAYLE, B. Control of cable-driven manipulators in the presence of friction. *Mechanism and machine theory*, v. 107, p. 139–147, 2017.

ALBUS, J.; BOSTELMAN, R.; DAGALAKIS, N. The nist robocrane. *Journal of Robotics System*, v. 10, n. 5, 1992.

AMRC, R. m. r. *Robot machining research*. 2018. <http://namrc.co.uk/centre/robot-machining-sae/>.

BALL, R. *A Treatise on the Theory of Screws, 1900*. [S.l.]: Cambridge University Press, Cambridge, UK, 1900.

BARRETTE, G.; GOSSELIN, C. M. Determination of the dynamic workspace of cable-driven planar parallel mechanisms. *Transactions of the ASME-R-Journal of Mechanical Design*, [New York, NY]: American Society of Mechanical Engineers,[c1990-, v. 127, n. 2, p. 242–248, 2005.

BLANDING, D. L. *Principles of exact constraint mechanical design*. [S.l.]: Eastman Kodak Company, 1992.

BOSSCHER, P. M. *Disturbance robustness measures and wrench-feasible workspace generation techniques for cable-driven robots*. Thesis (Doctorate) — Georgia Institute of Technology, 2004.

BRUCKMANN, T. *Auslegung und Betrieb redundanter paralleler Seilroboter*. Thesis (Doctorate) — Universität Duisburg-Essen, Fakultät für Ingenieurwissenschaften Maschinenbau und Verfahrenstechnik Institut für Mechatronik und Systemdynamik, 2010.

BRUCKMANN, T.; MIKELSONS, L.; BRANDT, T.; HILLER, M.; SCHRAMM, D. Wire robots part i: Kinematics, analysis & design. In: *Parallel manipulators, new developments*. [S.l.]: InTech, 2008.

BUTTOLO, P.; HANNAFORD, B. Advantages of actuation redundancy for the design of haptic displays. In: ASME. *Proceedings of the 1995 ASME International Mechanical Engineering Congress and Exposition*. [S.l.], 1995.

CAZANGI, H. R. Aplicação do método de davies para análise cinemática e estática de mecanismos com múltiplos graus de liberdade. Universidade

Federal de Santa Catarina, Centro Tecnológico, Programa de Pós-Graduação em Engenharia Mecânica, 2008.

CHASLES, M. Note sur les propriétés générales du système de deux corps semblables entr'eux et placés d'une manière quelconque dans l'espace; et sur le déplacement fini ou infiniment petit d'un corps solide libre. *Bulletin des Sciences Mathématiques, Férussac*, v. 14, p. 321–26, 1830.

COBOTS. 2018. <http://cobotsguide.com/>.

CONE, L. L. Skycam-an aerial robotic camera system. *Byte*, BYTE PUBL INC 70 MAIN ST, PETERBOROUGH, NH 03458, v. 10, n. 10, p. 122, 1985.

DAVIDSON, J. K.; HUNT, T. K. H. *Robots and Screw Theory: Applications of Kinematics and Statics to Robotics*. New York: Oxford University Press, 2004.

DAVIES, T. Kirchhoff's circulation law applied to multi-loop kinematic chains. *Mechanism and machine theory*, Elsevier, v. 16, n. 3, p. 171–183, 1981.

DIAO, X.; MA, O. A method of verifying force-closure condition for general cable manipulators with seven cables. *Mechanism and Machine Theory*, Elsevier, v. 42, n. 12, p. 1563–1576, 2007.

DUAN, B.; QIU, Y.; ZHANG, F.; ZI, B. Analysis and experiment of the feed cable-suspended structure for super antenna. In: IEEE. *Advanced Intelligent Mechatronics, 2008. AIM 2008. IEEE/ASME International Conference on*. [S.l.], 2008. p. 329–334.

FINOTELLO, R.; GRASSO, T.; ROSSI, G.; TERRIBILE, A. Computation of kinetostatic performances of robot manipulators with polytopes. In: IEEE. *Robotics and Automation, 1998. Proceedings. 1998 IEEE International Conference on*. [S.l.], 1998. v. 4, p. 3241–3246.

FIRMANI, F.; NOKLEBY, S. B.; ZIBIL, A.; PODHORODESKI, R. P. Wrench capabilities of planar parallel manipulators. part i: Wrench polytopes and performance indices. *Robotica*, Cambridge University Press, v. 26, n. 6, p. 791–802, 2008.

FRANTZ, J. C. *Análise Estática de Sistemas Robóticos Cooperativos*. Dissertação (Master) — Universidade Federal de Santa Catarina, 2015.

FRANTZ, J. C.; MEJIA, L.; SIMAS, H.; MARTINS, D. Analysis of wrench capability for cooperative robotic systems. In: *Proceedings of 23rd ABCM International Congress of Mechanical Engineering-COBEM*. [S.l.: s.n.], 2015.

GOSSELIN, C. Cable-driven parallel mechanisms: state of the art and perspectives. *Mechanical Engineering Reviews*, The Japan Society of Mechanical Engineers, v. 1, n. 1, p. DSM0004–DSM0004, 2014.

GOSSELIN, C.; ANGELES, J. A global performance index for the kinematic optimization of robotic manipulators. *Journal of Mechanical design*, American Society of Mechanical Engineers, v. 113, n. 3, p. 220–226, 1991.

GOSSELIN, C.; SEFRIOUI, J. Polynomial solutions for the direct kinematic problem of planar three-degree-of-freedom parallel manipulators. In: IEEE. *Advanced Robotics, 1991.'Robots in Unstructured Environments', 91 ICAR., Fifth International Conference on*. [S.l.], 1991. p. 1124–1129.

GOSSELIN, C. M.; JEAN, M. Determination of the workspace of planar parallel manipulators with joint limits. *Robotics and Autonomous Systems*, Elsevier, v. 17, n. 3, p. 129–138, 1996.

GOUGH, V. Contribution to discussion of papers on research in automobile stability, control and tyre performance. In: *Proc. Auto Div. Inst. Mech. Eng*. [S.l.: s.n.], 1956. v. 171, p. 392–394.

GOUTTEFARDE, M.; GOSSELIN, C. M. Analysis of the wrench-closure workspace of planar parallel cable-driven mechanisms. *IEEE Transactions on Robotics*, IEEE, v. 22, n. 3, p. 434–445, 2006.

GOUTTEFARDE, M.; MERLET, J.-P.; DANEY, D. Wrench-feasible workspace of parallel cable-driven mechanisms. In: IEEE. *Robotics and Automation, 2007 IEEE International Conference on*. [S.l.], 2007. p. 1492–1497.

J.E. Gwinnett. *Amusement device*. 1931. 1789680.

HUNT, K. H. Don't cross-thread the screw! *Journal of Field Robotics*, Wiley Online Library, v. 20, n. 7, p. 317–339, 2003.

HWANG, Y.-S.; LEE, J.; HSIA, C. A recursive dimension-growing method for computing robotic manipulability polytope. In: IEEE. *Robotics and Automation, 2000. Proceedings. ICRA'00. IEEE International Conference on*. [S.l.], 2000. v. 3, p. 2569–2574.

IRVINE, H. M.; IRVINE, M. *Cable structures*. [S.l.: s.n.], 1992.

KAWAMURA, S.; CHOE, W.; TANAKA, S.; PANDIAN, S. R. Development of an ultrahigh speed robot FALCON using wire drive system. *Proceedings - IEEE International Conference on Robotics and Automation*, v. 1, p. 215–220, 1995. ISSN 10504729.

KUMAR, V. R.; WALDRON, K. J. Force distribution in closed kinematic chains. *IEEE Journal on Robotics and Automation*, IEEE, v. 4, n. 6, p. 657–664, 1988.

LAFOURCADE, P.; LLIBRE, M.; REBOULET, C. Design of a parallel wire-driven manipulator for wind tunnels. In: QUEBEC CITY, CANADA. *Proceedings of the Workshop on Fundamental Issues and Future Research Directions for Parallel Mechanisms and Manipulators*. [S.l.], 2002. p. 187–194.

LANDSBERGER, S. E. A new design for parallel link manipulators. In: *Proceedings of the 1985 IEEE International Conference of Systems, Man and Cybernetics*. [S.l.: s.n.], 1985. p. 812–814.

LAU, D.; OETOMO, D.; HALGAMUGE, S. K. Wrench-closure workspace generation for cable driven parallel manipulators using a hybrid analytical-numerical approach. *Journal of Mechanical Design*, American Society of Mechanical Engineers, v. 133, n. 7, p. 071004, 2011.

MASLOW. *Maslow*. 2018. <http://www.maslowcnc.com/>.

MEJIA, L. *Otimização da capacidade de carga de um manipulador paralelo 3RRR simétrico em trajetórias com contato*. Dissertação (Master) — Universidade Federal de Santa Catarina, 2012.

MEJIA, L. *Wrench capability of planar manipulators*. Thesis (Doctorate) — Universidade Federal de Santa Catarina, 2016.

MEJIA, L.; FRANTZ, J.; SIMAS, H.; MARTINS, D. Modified scaling factor method for the obtention of the wrench capabilities in cooperative planar manipulators. In: *Proceedings of the 14th IFToMM World Congress*. [S.l.: s.n.], 2015. p. 572–581.

MEJIA, L.; SIMAS, H.; MARTINS, D. Force capability polytope of a 4rrr redundant planar parallel manipulator. In: *Advances in Robot Kinematics*. [S.l.]: Springer, 2014. p. 87–94.

MEJIA, L.; SIMAS, H.; MARTINS, D. Wrench capability in redundant planar parallel manipulators with net degree of constraint equal to four, five or six. *Mechanism and Machine Theory*, Elsevier, v. 105, p. 58–79, 2016.

MERLET, J.-P. Kinematics of the wire-driven parallel robot marionet using linear actuators. In: IEEE. *Robotics and Automation, 2008. ICRA 2008. IEEE International Conference on*. [S.l.], 2008. p. 3857–3862.

MERLET, J.-P.; GOSSELIN, C. Parallel mechanisms and robots. In: *Springer Handbook of Robotics*. [S.l.]: Springer, 2008. p. 269–285.

MING, A.; HIGUCHI, T. Study on multiple degree-of-freedom positioning mechanism using wires. i: Concept, design and control. *International Journal of the Japan Society for Precision Engineering*, Japan Society for Precision Engineering, v. 28, n. 2, p. 131–138, 1994.

MIURA, K.; FURUYA, H.; SUZUKI, K. Variable geometry truss and its application to deployable truss and space crane arm. *Acta Astronautica*, Elsevier, v. 12, n. 7-8, p. 599–607, 1985.

MURARO, T. Análise cinemática e estática de um mecanismo espacial atuado por cabos aplicado à movimentação de pacientes. Universidade Federal de Santa Catarina, Centro Tecnológico, Programa de Pós-Graduação em Engenharia Mecânica, 2015.

NAHON, M. A.; ANGELES, J. Real-time force optimization in parallel kinematic chains under inequality constraints. *IEEE Transactions on Robotics and Automation*, IEEE, v. 8, n. 4, p. 439–450, 1992.

NOKLEBY, S.; FIRMANI, F.; ZIBIL, A.; PODHORODESKI, R. Force-moment capabilities of redundantly-actuated planar-parallel architectures. In: *12th IFToMM 2007 World Congress*. [S.l.: s.n.], 2007. p. 17–21.

NOKLEBY, S.; FISHER, R.; PODHORODESKI, R.; FIRMANI, F. Force capabilities of redundantly-actuated parallel manipulators. *Mechanism and machine theory*, Elsevier, v. 40, n. 5, p. 578–599, 2005.

NUNES, W. M. Desenvolvimento de uma estrutura robótica atuada por cabos para reabilitação/recuperação dos movimentos do ombro humano. 2012.

PHAM, C. B.; YEO, S. H.; YANG, G.; KURBANHUSEN, M. S.; CHEN, I.-M. Force-closure workspace analysis of cable-driven parallel mechanisms. *Mechanism and Machine Theory*, Elsevier, v. 41, n. 1, p. 53–69, 2006.

POINSOT, L. *Théorie nouvelle de la rotation des corps*. [S.l.]: Bachelier, 1851.

POTT, A.; MEYER, C.; VERL, A. Large-scale assembly of solar power plants with parallel cable robots. In: VDE. *Robotics (ISR), 2010 41st International Symposium on and 2010 6th German Conference on Robotics (ROBOTIK)*. [S.l.], 2010. p. 1–6.

POTT, A.; MÜTHERICH, H.; KRAUS, W.; SCHMIDT, V.; MIERMEISTER, P.; VERL, A. Ipanema: a family of cable-driven parallel robots for industrial applications. In: *Cable-Driven Parallel Robots*. [S.l.]: Springer, 2013. p. 119–134.

PUSEY, J.; FATTAH, A.; AGRAWAL, S.; MESSINA, E. Design and workspace analysis of a 6–6 cable-suspended parallel robot. *Mechanism and machine theory*, Elsevier, v. 39, n. 7, p. 761–778, 2004.

SALISBURY, J. K. Active stiffness control of a manipulator in cartesian coordinates. In: IEEE. *Decision and Control including the Symposium on Adaptive Processes, 1980 19th IEEE Conference on*. [S.l.], 1980. v. 19, p. 95–100.

SCIAVICCO, L.; SICILIANO, B. Modelling and control of robot manipulators. *Measurement Science and Technology*, v. 11, n. 12, p. 1828, 2000. <http://stacks.iop.org/0957-0233/11/i=12/a=709>.

STEWART, D. A platform with six degrees of freedom. *Proceedings of the institution of mechanical engineers*, SAGE Publications Sage UK: London, England, v. 180, n. 1, p. 371–386, 1965.

SURDILOVIC, D.; BERNHARDT, R. String-man: a new wire robot for gait rehabilitation. In: IEEE. *Robotics and Automation, 2004. Proceedings. ICRA'04. 2004 IEEE International Conference on*. [S.l.], 2004. v. 2, p. 2031–2036.

TADOKORO, S.; VERHOEVEN, R.; HILLER, M.; TAKAMORI, T. A portable parallel manipulator for search and rescue at large-scale urban earthquakes and an identification algorithm for the installation in unstructured environments. In: IEEE. *Intelligent Robots and Systems, 1999. IROS'99. Proceedings. 1999 IEEE/RSJ International Conference on*. [S.l.], 1999. v. 2, p. 1222–1227.

TAO, J. M.; LUH, J. Coordination of two redundant robots. In: IEEE. *Robotics and Automation, 1989. Proceedings., 1989 IEEE International Conference on*. [S.l.], 1989. p. 425–430.

TRAVI, A. B. *Plataforma de Stewart Acionada por cabos*. Thesis (Doctorate) — Instituto Militar de Engenharia, 2009.

TSAI, L. *Mechanism Design: Enumeration of Kinematic Structures According to Function*. Boca Raton: CRC press, 2000. (Mechanical Engineering Series).

TSAI, L. W. *Robot Analysis: The Mechanics of Serial and Parallel Manipulators*. New York: Wiley, 1999. (Wiley-Interscience publication).

VERHOEVEN, R. *Analysis of the workspace of tendon-based Stewart platforms*. Thesis (Doctorate) — Universität Duisburg-Essen, Fakultät für Ingenieurwissenschaften» Maschinenbau und Verfahrenstechnik, 2004.

VISVANATHAN, V.; MILOR, L. S. An efficient algorithm to determine the image of a parallelepiped under a linear transformation. In: ACM. *Proceedings of the second annual symposium on Computational geometry*. [S.l.], 1986. p. 207–215.

WEIHMANN, L. *Modelagem e otimização de forças e torques aplicados por robós com redundância cinemática e de atuação em contato com o meio*. Thesis (Doctorate) — Universidade Federal de Santa Catarina, Centro Tecnológico, Programa de Pós-Graduação em Engenharia Mecânica, 2011.

WEIHMANN, L.; MARTINS, D.; COELHO, L.; BERNERT, D. Force capabilities of kinematically redundant planar parallel manipulators. In: *13th World Congress in Mechanism and Machine Science*. [S.l.: s.n.], 2011. p. 483–483.

WEIHMANN, L.; MARTINS, D.; COELHO, L. dos S. Modified differential evolution approach for optimization of planar parallel manipulators force capabilities. *Expert Systems with Applications*, Elsevier, v. 39, n. 6, p. 6150–6156, 2012.

YIN, X.; BOWLING, A. *The Robotics, Biomechanics, and Dynamic Systems Laboratory, University of Texas Arlington*. 2018. <http://loco.uta.edu/>.

YOSHIKAWA, T. Manipulability and redundancy control of robotic mechanisms. In: IEEE. *Robotics and Automation. Proceedings. 1985 IEEE International Conference on*. [S.l.], 1985. v. 2, p. 1004–1009.

ZIBIL, A.; FIRMANI, F.; NOKLEBY, S. B.; PODHORODESKI, R. P. An explicit method for determining the force-moment capabilities of redundantly actuated planar parallel manipulators. *Journal of mechanical design*, American Society of Mechanical Engineers, v. 129, n. 10, p. 1046–1055, 2007.

APPENDIX A – Screw Theory

The screw theory is a mathematical tool that is able to represent the instantaneous state of motions and actions of rigid bodies in space, being used at the kinematic and static analyses of manipulators. It is concerned primarily with the fundamental relationships among the degrees of freedom, the number of links, the number of joints, and the type of joints used in a mechanism (TSAI, 2000). It was first formulated by Mozzi (1763) and later systematized by Ball (1900). Nowadays the screw theory has been an important subject of study and found in mechanisms and robotics a fruitful field for its application (DAVIDSON; HUNT, 2004).

Chasles (1830) has proved that a free rigid body can be moved from any specified position to any other position by a movement consisting of a rotation around a straight line accompanied by a translation parallel to the straight line. However, Poinsot (1851) discovered that any system of forces which act upon a rigid body can be replaced by a single force and a couple in a plane perpendicular to the force. Thus, a force and its couple constitute an adequate representation of any system of forces applied to a rigid body (BALL, 1900).

Ball (1900) defines the *screw* as a geometrical element such as a point, plane or a line that is composed by a straight line, or axis, to which a scalar quantity of dimension, called *the pitch of the screw* (h) is added. Thus, Hunt (2003) exemplifies that in mechanics angular and translational velocity of a body combine as a *twist* on a *screw*; precisely analogously a force and a couple combine as a *wrench* on a *screw*.

The *screw* (\$) can be expressed by the six Plücker homogeneous coordinates (Eq. A.1), where $\vec{S}$ is the direction vector of the screw, $\vec{S_0}$ is the position vector of any point at the axis of the *screw* with respect to the origin of the coordinate system and L, M, N, P^*, Q^*, R^* are the Plücker homogeneous coordinates (CAZANGI, 2008).

$$\$ = \begin{pmatrix} \vec{S} \\ \hdashline \vec{S_0} \times \vec{S} + h\vec{S} \end{pmatrix} = \begin{pmatrix} L \\ M \\ N \\ \hdashline P^* = P + hL \\ Q^* = Q + hM \\ R^* = R + hN \end{pmatrix} \tag{A.1}$$

A.0.1 Motion Analysis

The instantaneous state of motion of a rigid body with respect to an inertial coordinate system O_{XYZ} can be represented by a screw called

twist $\$^M$. It is composed by an angular differential velocity ω around the instantaneous rotation screw axis and a translational differential velocity v coincident with the same axis. Equation A.2 shows how to define the screw pitch with respect to the body velocities. Equation A.3 represents how the Plücker homogeneous coordinates from equation A.1 can be rewritten as six motion coordinates (CAZANGI, 2008).

$$h = \frac{v}{\omega} \tag{A.2}$$

$$\$^M = \begin{pmatrix} \mathscr{L} \\ \mathscr{M} \\ \mathscr{N} \\ \hline \mathscr{P}^* = \mathscr{P} + h\mathscr{L} \\ \mathscr{Q}^* = \mathscr{Q} + h\mathscr{M} \\ \mathscr{R}^* = \mathscr{R} + h\mathscr{N} \end{pmatrix} = \begin{pmatrix} \vec{\omega} \\ \hline \vec{S}_0 \times \vec{\omega} + h\vec{\omega} \end{pmatrix} = \begin{pmatrix} \vec{\omega} \\ \hline \vec{V}_P \end{pmatrix} \tag{A.3}$$

The first three components are related to the angular velocities $\vec{\omega}$ by $\sqrt{\mathscr{L}^2 + \mathscr{M}^2 + \mathscr{N}^2} = |\vec{\omega}|$. The last three components represents the linear velocity $\vec{V}_P$ of a point P at the rigid body that instantaneously coincident with the origin O_{XYZ} and is obtained by $\sqrt{(\mathscr{P}^*)^2 + (\mathscr{M}^*)^2 + (\mathscr{N}^*)^2} = |\vec{V}_P|$ (CAZANGI, 2008).

The *screw twist* $\$^M$ can be normalized in a geometric element $\hat{\$}^M$ without any associated mechanical magnitude and a scalar amplitude (φ) with an angular velocity magnitude (CAZANGI, 2008).

$$\$^M = \begin{pmatrix} \vec{\omega} \\ \hline \vec{S}_0 \times \vec{\omega} + h\vec{\omega} \end{pmatrix} = \begin{pmatrix} \vec{S}^M \varphi \\ \hline (\vec{S}_O \times \vec{S}^M + h\vec{S}^M)\varphi \end{pmatrix} \tag{A.4}$$

$$\$^M = \begin{pmatrix} \vec{S}^M \\ \hline \vec{S}_O \times \vec{S}^M + h\vec{S}^M \end{pmatrix} \varphi = \hat{\$}^M \varphi \tag{A.5}$$

Where $\vec{S}^M$ is the vector of unit directions L, M, N (director cosines) of the normalized twist, associated by $L^2+M^2+N^2=1$. The magnitude is $\varphi = |\vec{\omega}|$. Some values of the *screw pitch* can lead to particular conditions. A pure rotation is represented by the *screw pitch* (h) zero, with $v=0$ and $\vec{V}_P = \vec{S}_0 \times \vec{\omega}$.

$$\$^M = \begin{pmatrix} \mathscr{L} \\ \mathscr{M} \\ \mathscr{N} \\ \hline \mathscr{P} \\ \mathscr{Q} \\ \mathscr{R} \end{pmatrix} = \begin{pmatrix} \vec{\omega} \\ \hline \vec{S}_0 \times \vec{\omega} \end{pmatrix} = \begin{pmatrix} \vec{S}^M \\ \hline \vec{S}_0 \times \vec{S}^M \end{pmatrix} \varphi \tag{A.6}$$

A pure translation happens when the *screw pitch* value is infinite, the angular velocity $\vec{\omega} = 0$ leading to the *screw twist*:

$$\$^M = \begin{pmatrix} 0 \\ 0 \\ 0 \\ \hline \mathscr{P}^* \\ \mathscr{Q}^* \\ \mathscr{R}^* \end{pmatrix} = \begin{pmatrix} \vec{0} \\ \hline v \end{pmatrix} = \begin{pmatrix} \vec{0} \\ \hline \vec{S}^M \end{pmatrix} \varphi \tag{A.7}$$

The relative movement of a system of two bodies (i) and (j) in motion, with respect to the same inertial referential, can be obtained by the superposition of its *screw twists*. If there is a coupling (a) between the bodies (i) and (j) represented by the *screw twist* $\$_a^M$, the relative motion can be obtained by the sum of the *screw twists* $\$_i^M$ and $\$_j^M$, as follows:

$$\$_a^M = \$_{ij}^M = \$_i^M + \$_j^M . \tag{A.8}$$

A.0.1.1 Motion Matrix $[M_D]_{\lambda \times F}$

All the *screw twists* of a mechanism can be represented by a single *Matrix of Motion* $[M_D]_{\lambda \times F}$. The number of rows of this matrix is obtained by the order of the system (λ) and the columns represents the unitary motions of each joint (CAZANGI, 2008).

$$[M_D]_{\lambda \times F} = \begin{bmatrix} \$_a^M & \$_b^M & \$_c^M & \ldots & \$_F^M \end{bmatrix} \tag{A.9}$$

Also, the *matrix of motions* can be represented as a *matrix of unitary*

motions $[M_D]_{\lambda\times F}$ that is composed by the normalized *screw twists* and a *vector of motion magnitudes*.

$$[M_D]_{\lambda\times F} = \begin{bmatrix} \hat{\$}_a^M & \hat{\$}_b^M & \hat{\$}_c^M & \dots & \hat{\$}_F^M \end{bmatrix} \tag{A.10}$$

The motion magnitudes are organized into a single *vector of motion magnitudes* $\{\vec{\phi}_{F\times 1}\}$.

$$\vec{\phi}_{F\times 1} = \begin{Bmatrix} \varphi_a \\ \varphi_b \\ \vdots \\ \varphi_F \end{Bmatrix} \tag{A.11}$$

A.0.2 Action Analysis

The state of actions of a rigid body, with respect to an inertial coordinate system O_{XYZ}, can be represented by a *screw wrench* ($\$^A$). It is composed by a vector who represents the resultant force ($\vec{R}$), whose line of action coincides with the screw axis, and a binary ($\vec{T}$) parallel to the referred axis. The binary ($\vec{T}$) has units of $[force]\times[\ length\ ]$ and can be related to the resultant by an scalar parameter the *screw pitch* (h) as shown in Eq. A.12 (BALL, 1900; CAZANGI, 2008).

$$\vec{T} = h\vec{R} \tag{A.12}$$

Analogously to the motion analysis, the Plücker homogeneous coordinates can be rewritten as six action coordinates, as show in Eq. A.13. The first three components represents the binary $\vec{T}_P$ that acts over the rigid body in a point P that is instantaneously coincident with the origin O_{xyz} and can be obtained by $\sqrt{\mathscr{P}^* + \mathscr{Q}^* + \mathscr{R}^*} = |\vec{T}_P|$. The last three components represents the resultant force $\vec{F}$ and can be obtained by $\sqrt{\mathscr{L}^* + \mathscr{M}^* + \mathscr{N}^*} = |\vec{R}|$ (CAZANGI, 2008).

$$\$^A = \begin{pmatrix} \mathscr{P}^* = \mathscr{P} + h\mathscr{L} \\ \mathscr{Q}^* = \mathscr{Q} + h\mathscr{M} \\ \mathscr{R}^* = \mathscr{R} + h\mathscr{N} \\ \hdashline \mathscr{L} \\ \mathscr{M} \\ \mathscr{N} \end{pmatrix} = \begin{pmatrix} \vec{S}_0 \times \vec{R} + h\vec{R} \\ \hdashline \vec{R} \end{pmatrix} = \begin{pmatrix} \vec{T}_P \\ \hdashline \vec{R} \end{pmatrix} \tag{A.13}$$

The normalization of the *screw wrench*($\$^A$) leads to a geometrical element $\hat{\$}^A$ without any associated mechanical unit and a magnitude ψ with force units, as presented in Eq. A.15. Regarding the *screw pitch*, as happened in the motion analysis, there are two particular conditions. Thus, a *screw pitch* (h) zero, leads to a state of pure force at the *screw wrench*. As opposed to, a *screw pitch* infinite represents a state of pure torque at the *wrench*:

$$\$^A = \begin{pmatrix} \vec{S}_0 \times \vec{R} + h\vec{R} \\ \text{- - - - - - - - -} \\ \vec{R} \end{pmatrix} = \begin{pmatrix} (\vec{S}_0 \times \vec{S}^A + h\vec{S}^A)\psi \\ \text{- - - - - - - - - - - -} \\ \vec{S}^A \psi \end{pmatrix} \tag{A.14}$$

$$\$^A = \begin{pmatrix} (\vec{S}_0 \times \vec{S}^A + h\vec{S}^A) \\ \text{- - - - - - - - - - -} \\ \vec{S}^A \end{pmatrix} \psi = \hat{\$}^A \psi \tag{A.15}$$

A.0.2.1 Action Matrix $[A_D]_{\lambda \times C}$

Similarly to the *motion matrix*, all the *screw wrenches* of a mechanism can be disposed into a single *matrix of actions*. Thus, the number of rows of this matrix is obtained by the system order (λ) and the columns represent the unitary restrictions of each joint by *screw wrenches*.

$$[A_D]_{\lambda \times C} = \begin{bmatrix} \$_a^A & \$_b^A & \dots & \$_C^A \end{bmatrix} \tag{A.16}$$

Thus, this matrix can be represented as a matrix of unitary actions $[A_D]_{\lambda \times C}$ that is composed by the normalized *screw wrenches*.

$$[A_D]_{\lambda \times C} = \begin{bmatrix} \hat{\$}_a^A & \hat{\$}_b^A & \dots & \hat{\$}_C^A \end{bmatrix} \tag{A.17}$$

The magnitudes composes the *vector of action magnitudes* $\{\vec{\Psi}\}_{C \times 1}$:

$$\vec{\Psi}_{C\times 1} = \begin{Bmatrix} \psi_a \\ \psi_b \\ \vdots \\ \psi_C \end{Bmatrix}. \tag{A.18}$$

A.0.3 Kirchhoff circuit laws

As presented before, Davies has used the Kirchhoff circulation laws for electrical networks to build an analogy to mechanical systems. Thus, the *kinematic analysis* is done by an adaptation of the *Kirchhoff voltage law* that is applied for closed loops. In addition, the *static analysis* is obtained by an adaptation of the *Kirchhoff current law* that is applied to nodes (CAZANGI, 2008).

A.0.3.1 Motions in a circuit

The *Kirchhoff voltage law* defines that the algebraic sum of voltages that acts in a closed loop is always zero. Analogously, Davies (1981) establishes that the *algebraic sum of screw wrenches that acts in the same loop is always zero*, being called the *circuit law*. Thus, for any closed sequence of bodies in relative motion to each other the sum of each motion coordinate is null. As a result, a mechanism that is moving in space (order $\lambda = 6$) has:

$$\sum \mathscr{L} = \sum \mathscr{M} = \sum \mathscr{N} = \sum \mathscr{P}^* = \sum \mathscr{Q}^* = \sum \mathscr{R}^* = 0 \tag{A.19}$$

Applying the matrix notation (Eqs. A.9, A.11 and A.10) leads to:

$$\sum \$^M \equiv [M_D]_{\lambda\times F} = [\hat{M}_D]_{\lambda\times F}\{\vec{\Psi}\}_{F\times 1} = \{\vec{0}\}_{\lambda\times 1} \tag{A.20}$$

A.0.3.2 Actions in a cutset

The *Kirchhoff current law* establishes that an algebraic sum of currents flowing into and out of a node is always zero. Analogously, Davies (1981) defines that the algebraic sum of *screw wrenches* that acts at the same cutset is always zero, being called the *Cutset Law* (CAZANGI, 2008).

This implies that, for any system of connected bodies that are in

equilibrium, there is a subset of couplings separated by a cutset where the sum of each coordinate of action of this couplings is null. Thus, for a cutset in space (order $\lambda = 6$):

$$\sum \mathscr{P}^* = \sum \mathscr{Q}^* = \sum \mathscr{R}^* \sum = \mathscr{L} = \sum \mathscr{M} = \sum \mathscr{N} = 0 \tag{A.21}$$

Applying the matrix notation leads to:

$$\sum \$^A \equiv [A_D]_{\lambda \times C} = [\hat{A}_D]_{\lambda \times C} \{\vec{\Psi}\}_{C \times 1} = \{\vec{0}\}_{\lambda \times 1} \tag{A.22}$$

A.0.4 Determination of the equation system

As seen before, the fundamental circuits and cuts are subsets of the independent edges in a graph and can be represented mathematically by the matrix of circuits $[B]$ and the matrix of cutsets $[Q]$. Thus, for a mechanism with one or more circuits, it is possible to determine a system of equations for kinematics using the Eq. A.20 and the circuits of a kinematic chain's graph. Analogously, for a mechanism with one or more cuts, it is possible to define a system of equations for statics using the Eq. A.22 and the f-cutsets of kinematic chain's graph (CAZANGI, 2008).

A.0.4.1 Kinematics: network of unitary motions matrix $[\hat{M}_N]_{\lambda.l \times F}$

A network of couplings with l fundamental circuits at the space of order λ can be represented as a set of $\lambda \times l$ equations that defines the conditions that must be satisfied by F unknowns. The circuits determine the topological relations between the unknowns that are contained in each coupling *screw twist* (CAZANGI, 2008).

The definition of the *network of unitary motions matrix* $[\hat{M}_N]_{\lambda.l \times F}$ may be done by the distribution of the normalized *twists* that belongs to each circuit, multiplying the *matrix of unitary motions* $[\hat{M}_D]_{\lambda \times F}$ by each line of the matrix of circuits-f $[B_M]_{l \times F}$.

$$[B_{M_i}]_{1 \times F} = \begin{bmatrix} B_{M_{i,1}} & B_{M_{i,2}} & B_{M_{i,1}} & \cdots & B_{M_{i,F}} \end{bmatrix}_{1 \times F} \tag{A.23}$$

$$diag\{[B_{M_i}]_{1\times F}\} = \begin{bmatrix} B_{M_{i,1}} & 0 & \cdots & B_{M_{i,F}} \\ 0 & B_{M_{i,2}} & \cdots & B_{M_{i,F}} \\ & & \ddots & \\ 0 & 0 & \cdots & B_{M_{i,F}} \end{bmatrix}_{F\times F} \tag{A.24}$$

$$[\hat{M}_N]_{\lambda.l\times F} = \begin{bmatrix} [\hat{M}_D]_{\lambda\times F}.diag\{[B_{M_1}]_{1\times F}\} \\ [\hat{M}_D]_{\lambda\times F}.diag\{[B_{M_2}]_{1\times F}\} \\ \vdots \\ [\hat{M}_D]_{\lambda\times F}.diag\{[B_{M_l}]_{1\times F}\} \end{bmatrix}_{\lambda.l\times F} \tag{A.25}$$

The *circuit law* requires that each of the λ components of the *screw twist* that belongs to a circuit has sum equal zero. Thus, the matrix $[\hat{M}_N]_{\lambda.l\times F}$ multiplied by the vector of unknowns of motion magnitudes $\{\Phi\}_{F\times 1}$ is equal to zero, building the *system of kinematics equations* (CAZANGI, 2008).

$$[\hat{M}_N]_{\lambda.l\times F}\{\Phi\}_{F\times 1} = \{\vec{0}\}_{\lambda.l\times 1} \tag{A.26}$$

The F unknowns associated by $\lambda.l$ equations can be rewritten as function of a subset of F_N unknowns (primary variables), where F_N is the *net degree of freedom* of the kinematic chain. Thus, it is possible to claim that the movement of the kinematic chain is determined by the definition of F_N unknowns of magnitudes of $\{\vec{\Phi}\}_{F\times 1}$.

A.0.4.2 Action: network of unitary actions matrix $[\hat{A}_N]_{\lambda.k\times C}$

A system with $\lambda.k$ equations may be used to represent an over-constrained kinematic chain with k f-cutsets in a space of order λ. In this case, the system of equations shows the conditions that may be satisfied by C unknowns, whereas the cutset-f defines the topological relations between the unknowns that are contained in the *screw wrenches* of each coupling (CAZANGI, 2008).

The construction of the *network of unitary actions matrix* $[\hat{A}_N]_{\lambda.k\times C}$ it is possible through the distribution of normalized *wrenches* that belongs to each cutset, multiplying the *matrix of unitary actions* $[\hat{A}_D]_{\lambda\times C}$ by each line of the *cutset-f matrix* $[Q_A]_{k\times C}$ (CAZANGI, 2008).

As presented before, to achieve algebraic consistency, k diagonal matrices of $[Q_A]_{\lambda.k\times C}$, where each line $i = 1,2,...,k$ has its elements arranged at the main diagonal. Thus, the following equations shows the algebraic

procedure to build $[\hat{A}_N]_{\lambda.k\times C}$

$$[Q_{A_i}]_{1\times F} = \begin{bmatrix} Q_{A_{i,1}} & Q_{A_{i,2}} & Q_{A_{i,1}} & \cdots & Q_{A_{i,C}} \end{bmatrix}_{1\times C} \tag{A.27}$$

$$diag\{[Q_{A_i}]_{1\times C}\} = \begin{bmatrix} Q_{A_{i,1}} & 0 & \cdots & B_{M_{i,C}} \\ 0 & Q_{A_{i,2}} & \cdots & B_{M_{i,C}} \\ & & \ddots & \\ 0 & 0 & \cdots & Q_{A_{i,C}} \end{bmatrix}_{C\times C} \tag{A.28}$$

$$[\hat{A}_N]_{\lambda.k\times C} = \begin{bmatrix} [\hat{A}_D]_{\lambda\times C}.diag\{[Q_{A_1}]_{1\times C}\} \\ [\hat{A}_D]_{\lambda\times C}.diag\{[Q_{A_2}]_{1\times C}\} \\ \vdots \\ [\hat{A}_D]_{\lambda\times C}.diag\{[Q_{A_l}]_{1\times C}\} \end{bmatrix}_{\lambda.l\times C} \tag{A.29}$$

The *cutset law* requires that each of the λ components of the *screw wrench* that belongs to a subset of rigid bodies in equilibrium, determined by a cutset, has sum equal zero.

Thus, the matrix $[\hat{A}_N]_{\lambda.k\times F}$ multiplied by the vector of unknowns of action magnitudes $\{\vec{\Psi}\}_{C\times 1}$ is equal to zero, building the *system of static equations* (CAZANGI, 2008).

$$[\hat{A}_N]_{\lambda.k\times F}\{\vec{\Psi}\}_{C\times 1} = \{\vec{0}\}_{\lambda.k\times 1} \tag{A.30}$$

The C unknowns organized through $\lambda \times k$ equations can be rewritten in function of the subset of C_N unknowns (primary variables), where C_N is the *net degree of restriction* of the over-constrained kinematic chain. Thus, it is possible to determine the internal actions of the kinematic chain by the imposition of the C_N variables of magnitudes of $\{\vec{\Psi}\}_{C\times 1}$ (CAZANGI, 2008).

A.0.5 Solution of the equation system

Once identified the primary variables in the magnitude vectors, it is possible to split the system into two subsets: the primary variables (knowns), identified by the subscript P, and the secondary variables (unknowns) identified by the subscript S. As a result, the net matrices and the magnitude vectors may be reorganized to determine the solution of the systems.

A.0.5.1 Kinematics solution $\{\vec{\Phi}_S\}_{m\times 1}$.

The kinematics equation system is partitioned into F_N primary variables and m secondary variables and rearranged as follows (CAZANGI, 2008):

$$\left[\begin{array}{c|c} [\hat{M}_{NS}]_{m\times m} & [\hat{M}_{NP}]_{m\times F_N} \end{array}\right] \left\{ \begin{array}{c} \{\hat{\Phi}_S\}_{m\times 1} \\ \hline \{\hat{\Phi}_P\}_{F_N\times 1} \end{array} \right\} = \{\vec{0}\}_{m\times 1} \therefore \tag{A.31}$$

$$[\hat{M}_{NS}]_{m\times m}\{\hat{\Phi}_S\}_{m\times 1} + [\hat{M}_{NP}]_{m\times F_N}\{\hat{\Phi}_P\}_{F_N\times 1} = \{\vec{0}\}_{m\times 1} \therefore \tag{A.32}$$

$$[\hat{M}_{NS}]_{m\times m}\{\hat{\Phi}_S\}_{m\times 1} = -[\hat{M}_{NP}]_{m\times F_N}\{\hat{\Phi}_P\}_{F_N\times 1} \tag{A.33}$$

The last step is to isolate the vector of variables $\{\hat{\Phi}_S\}_{m\times 1}$, inverting the matrix of secondary variables, which leads to the *kinematics solution*, as presented in Eq. A.34. Finally, the solution of the system $\{\hat{\Phi}_S\}_{m\times 1}$ is obtained by coherent values of the primary variables $\{\hat{\Phi}_P\}_{F_N\times 1}$.

$$\{\hat{\Phi}_S\}_{m\times 1} = -[\hat{M}_{NS}]^{-1}_{m\times m}[\hat{M}_{NP}]_{m\times F_N}\{\hat{\Phi}_P\}_{F_N\times 1} \tag{A.34}$$

A.0.5.2 Statics solution $\{\vec{\Psi}\}_{a\times 1}$.

Similarly to the kinematics analysis, the system of statics equations can be divided into C_N primary variables and a secondary variables and rearranged as follows (CAZANGI, 2008):

$$\left[\begin{array}{c|c} [\hat{A}_{NS}]_{a\times a} & [\hat{A}_{NP}]_{a\times C_N} \end{array}\right] \left\{ \begin{array}{c} \{\hat{\Psi}_S\}_{a\times 1} \\ \hline \{\hat{\Psi}_P\}_{C_N\times 1} \end{array} \right\} = \{\vec{0}\}_{a\times 1} \therefore \tag{A.35}$$

$$[\hat{A}_{NS}]_{a\times a}\{\hat{\Psi}_S\}_{a\times 1} + [\hat{A}_{NP}]_{a\times C_N}\{\hat{\Psi}_P\}_{C_N\times 1} = \{\vec{0}\}_{a\times 1} \therefore \tag{A.36}$$

$$[\hat{A}_{NS}]_{a\times a}\{\hat{\Psi}_S\}_{a\times 1} = -[\hat{A}_{NP}]_{a\times C_N}\{\hat{\Psi}_P\}_{C_N\times 1} \tag{A.37}$$

Further, the last step is to isolate the variables vector $\{\hat{\Psi}_S\}_{a\times 1}$, inverting the matrix of secondary variables, which leads to the *statics*

solution.

$$\{\hat{\Psi}_S\}_{a\times 1} = -[\hat{A}_{NS}]^{-1}_{a\times a}[\hat{A}_{NP}]_{a\times C_N}\{\hat{\Psi}_P\}_{C_N\times 1} \tag{A.38}$$

Finally, the solution is obtained by applying coherent values to the primary variables.

A.1 STATICS OF CABLE ROBOTS

The static analysis of cable robots (Fig. 53) through the *Davies' Method* requires the definition of a cables' kinematic model using conventional joints and rigid links. Thus, this configuration must held the same kinematic properties as the regular configuration with cables, that is, six and three degrees of freedom in space and plan, respectively. The spatial configuration is done by a prismatic joint connected to the base by a spherical joint and to the platform by a universal joint. In a planar configuration, the spherical and universal joints are replaced by rotative joints. The planar configuration is represented schematically in Fig. 53b.

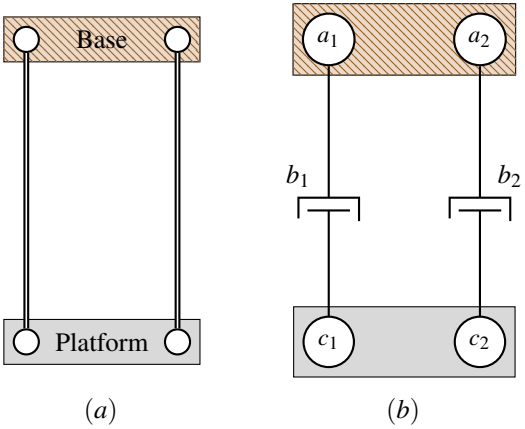

Figure 53: Cable robot with 2 limbs (a) schematic representation and (b) equivalent kinematic model with two prismatic and four rotational joints.

Further, cable robots kinematic models may be named as conventional parallel structures using the nomenclature proposed by Tsai (2000). In this case, a code with a number, that represents the number of limbs, and three letters, defining the types of joints that composes the mechanism, was

employed. Furthermore, an underline is used to represent the actuated joint of the limb. Thus, Fig. 53b shows a 2-R$\underline{\text{P}}$R robot.

After the definition of the cable robot kinematic configuration, following the steps proposed by Cazangi (2008), all the actions (*torques and forces*) of the manipulator joints must be defined. To this end, Fig. 54 shows the actions at the 2-R$\underline{\text{P}}$R manipulator. Firstly, since the actuation of a cable robot corresponds to changes in the length of the cable by a motor, the actuation that represents better this behaviour is a force alongside the axis of the prismatic joint, represented by forces in x and y in each prismatic joint. Secondly, cables are able to rotate freely in a plan, thus, the rotative joints must allow the kinematic chain to rotate freely offering only reaction forces in x and y. Finally, a torque in the prismatic joint is also presented, since this component will not allow any rotation between its adjacent links.

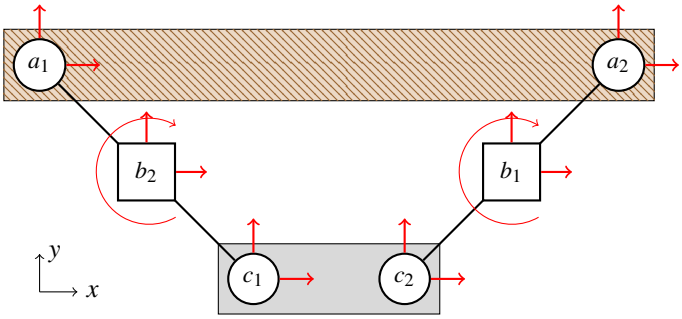

Figure 54: Actions at the 2-R$\underline{\text{P}}$R joints.

The 2-R$\underline{\text{P}}$R mechanism may also be represented by a directed graph (Fig. 55). In this case, the joints are represented by edges and the rigid bodies by vertices. The direction of each edge was chosen to simplify the next steps of the *Davies' Method*: all the joints' actions go from the fixed base to the movable platform, which is the usual force directions in the actuation of parallel manipulators. Additionally, an edge (d), representing the external forces and torques that act between the movable platform and the fixed base, is added to the mechanism graph. The *spanning tree* of this graph is also presented in Fig. 55. The dashed edges shows the chords while the black edges compose the tree.

Futhermore, all the actions at the mechanism are summarized in Fig. 56. After the definition of the graph and the action edges it is possible to define the fundamental circuits and cutsets of this graph. The red dashed lines in Fig. 56 represent five possible cutsets in the 2-R$\underline{\text{P}}$R graph. Likewise the fundamental circuits(v_1 and v_2) are represented by dashed lines.

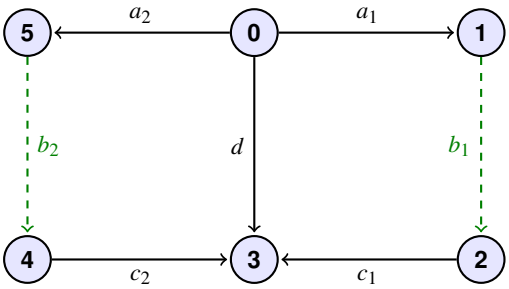

Figure 55: Directed Graph - 2-RPR Robot

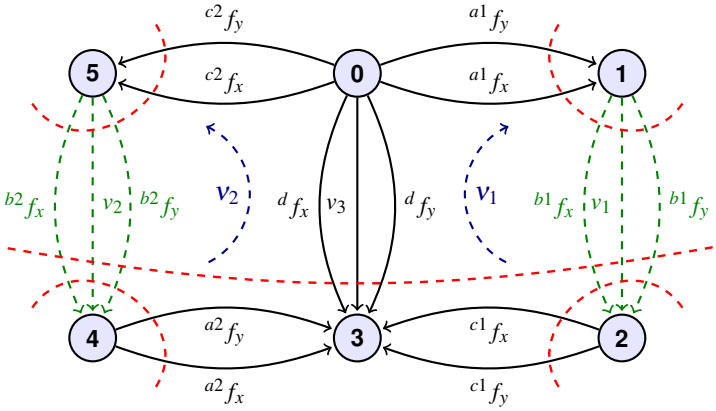

Figure 56: Actions Graph - 2-RPR Robot

As presented before, after the definition of the fundamental cutsets, it is possible to define the *cutset matrix* $[Q_a]$(Eq. A.39).

$$[Q_a]_{5\times 7} = \begin{array}{c} \begin{matrix} a_1 & b_1 & c_1 & a_2 & b_2 & c_2 & d \end{matrix} \\ \begin{bmatrix} 1 & -1 & 0 & 0 & 0 & 0 & 0 \\ 0 & -1 & 1 & 0 & 0 & 0 & 0 \\ 0 & 0 & 0 & 1 & -1 & 0 & 0 \\ 0 & 0 & 0 & 0 & -1 & 1 & 0 \\ 0 & 1 & 0 & 0 & 1 & 0 & 1 \end{bmatrix} \end{array} \begin{matrix} \\ \text{cutset}_{a_1} \\ \text{cutset}_{c_1} \\ \text{cutset}_{a_2} \\ \text{cutset}_{c_2} \\ \text{cutset}_{d} \end{matrix} \tag{A.39}$$

Since this analysis is focused on planar robots the order of the screw

system (λ) can be reduced to three. In this case, only forces f_x and f_y and a moment M_z acts on the manipulator joints. The representation of the simplified wrench is presented at Eq. A.40. Further, y_{a_1} and x_{a_1} represents the coordinates of the a_1 joint.

$$\$_{a_1} = \begin{bmatrix} -y_{a_1} \\ 1 \\ 0 \end{bmatrix} {}^{a_1}f_x + \begin{bmatrix} x_{a_1} \\ 0 \\ 1 \end{bmatrix} {}^{a_1}f_y + \begin{bmatrix} 1 \\ 0 \\ 0 \end{bmatrix} {}^{a_1}M_z \tag{A.40}$$

Additionally, the matrix of unitary actions $[\hat{A}_D]_{\lambda \times C}$ can be obtained by the *normalized screw wrenches*.

$$[A_D]_{\lambda \times C} = \begin{bmatrix} \hat{\$}^A_{a_1} & \hat{\$}^A_{b_1} & \hat{\$}^A_{c_1} & \hat{\$}^A_{a_2} & \hat{\$}^A_{b_2} & \hat{\$}^A_{c_2} & \hat{\$}^A_{d} \end{bmatrix} \tag{A.41}$$

Thus, the *vector of action magnitudes* $\{\vec{\Psi}\}_{C\times 1}$ is obtained by all the actions that are represented in the Fig. 54.

$$\{\vec{\Psi}\}_{17\times 1} = \begin{Bmatrix} {}^{a_1}f_x \\ {}^{a_1}f_y \\ {}^{b_1}f_x \\ \vdots \\ {}^{c_2}f_x \\ {}^{c_2}f_y \\ {}^{d}f_x \\ {}^{d}f_y \\ {}^{d}M_z \end{Bmatrix} \tag{A.42}$$

Furthermore, concluded the definition of each joint's *wrench* it is possible to build the *action matrix*. To do so, each *wrench* must be inserted in the respective element of the cutset matrix while the remained spaces may be filled with zeros.

$$[\hat{A}_N]_{15\times 17} = \begin{array}{c} \begin{matrix} a_1 & b_1 & c_1 & a_2 & b_2 & c_2 & d \end{matrix} \\ \begin{bmatrix} \hat{\$}_{a_1} & -\hat{\$}_{b_1} & 0 & 0 & 0 & 0 & 0 \\ 0 & -\hat{\$}_{b_1} & \hat{\$}_{c_1} & 0 & 0 & 0 & 0 \\ 0 & 0 & 0 & \hat{\$}_{a_2} & -\hat{\$}_{b_2} & 0 & 0 \\ 0 & 0 & 0 & 0 & -\hat{\$}_{b_2} & \hat{\$}_{c_2} & 0 \\ 0 & \hat{\$}_{b_1} & 0 & 0 & \hat{\$}_{b_2} & 0 & \hat{\$}_{d} \end{bmatrix} \end{array} \tag{A.43}$$

Finally, the matrix $[\hat{A}_N]$ multiplied by the vector of action magnitudes

$\{\vec{\Psi}\}$ is equal to zero allowing to obtain the solution of the equation system.

$$[\hat{A}_N]_{15\times17}\{\vec{\Psi}\}_{1\times17} = \{\vec{0}\} \tag{A.44}$$

Further, the *jacobian matrix* (**J**) is needed to defined the *force capability*.Thus, the primary and secondary variables must be organized allowing to obtain the forces in the mobile platform based on the actuator forces (Eq. A.45).

$$\{F_{ext}\} = [\mathbf{J}]\{v\} \tag{A.45}$$

Furthermore, the external forces are represented by d and must be defined as secondary variables. In addition, the variables that represents the forces in the robot joints must be defined as primary variables. Thus, Eq. A.46 shows how the solution of the equation system can be obtained dividing the $\hat{A}_N$ in $\hat{A}_{NP}$ (elements that multiply the primary variables) and $\hat{A}_{NS}$ (elements that multiply the secondary variables).

$$\begin{Bmatrix} {}^{d}f_x \\ {}^{d}f_y \\ {}^{d}M_z \end{Bmatrix} = -[\hat{A}_{NS}]^{-1}_{15\times3}[\hat{A}_{NP}]_{15\times14} \begin{Bmatrix} {}^{a_1}f_x \\ \vdots \\ {}^{c_2}f_y \end{Bmatrix} \tag{A.46}$$

Finally, since only the actions on the actuated joints are needed to define the *jacobian matrix*, just the lines that multiply the forces in the joints b_1 and b_2 are taken from Eq. A.46 to build the jacobian.

$$\begin{Bmatrix} {}^{d}f_x \\ {}^{d}f_y \end{Bmatrix} = [J] \begin{Bmatrix} {}^{b_1}f_x \\ {}^{b_1}f_y \\ {}^{b_2}f_x \\ {}^{b_2}f_y \end{Bmatrix} \tag{A.47}$$

A.2 EXACT CONSTRAINTS AND NESTING FORCES

Blanding (1992) defines the concept of *exact constraint* as a principle for machine design that could lead to more efficient and low cost machines. First, as presented in Chapter 3, the concept defines the number of degrees of freedom that a connection imposes to the body that its restrain. According to Blanding (1992), the design of mechanical connections between parts of a device must account for the exact required amount of DoFs of each body in a mechanism avoiding overconstrains and underconstraints, since this could lead to undesired forces and moments in the assembly of mechanical devices or undesired DoFs.

In our case, the concept of *exact constraint* will be used to analyse the mobile platform behaviour of cable driven parallel robots. As presented before, a rigid body is able to perform two translations and one rotation (Fig. 57a) in a space with two dimensions (2D), thus, its exact constraint requires the constraint of three degrees of freedom. First, a rigid link with two rotative joins can be used to restrain one DoF of rigid body in plane. Thus, the body of Fig. 57b remains able to translate alongside y and rotate about z.

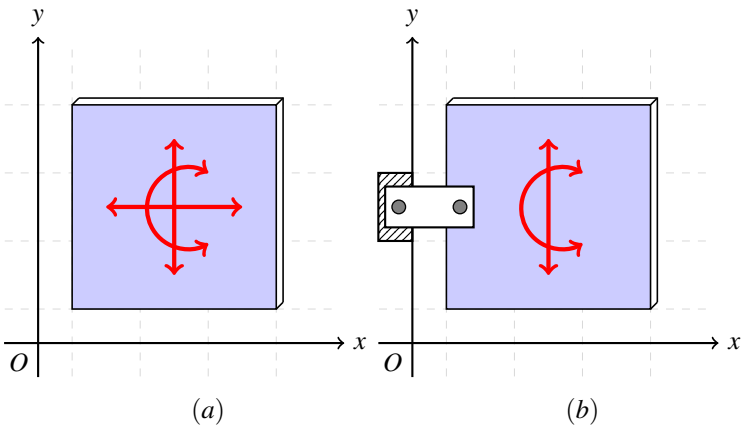

Figure 57: Motions in a two-dimensional space.

Blanding (1992) also introduces the concept of *nesting force* as a magnitude that will ensure that contact is maintained between two objects. As an example, a book is on the table because gravity is acting as a *nesting force*. Thus, the constraint that is presented in Fig. 57b could also be done by a *nesting force* (n_{nf}) in x-direction and a post (Fig. 58a). Additionally,

Fig. 58b shows an example of overconstraint. In this case, since the action line of the two constraints are parallel, they lead to an overconstraint which imposes that the size of the constrained body must be exactly the gap between the posts or the parts will not fit properly. This leads to practical difficulties, that could be avoided by the use of a spring instead of one of the posts.

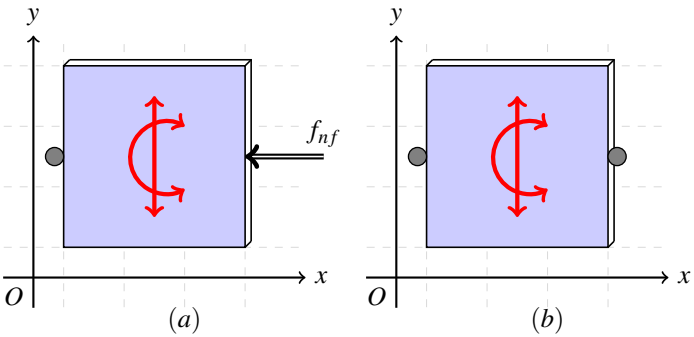

Figure 58: Constraint by a post and a nesting force f_{nf}.

According to Blanding (1992), the *constraint line* defines the *instant center of rotation* or *virtual pivot point* of a constrained body. Thus, since two parallel lines does not define a *virtual pivot point*, parallel constraint lines leads to overconstraint of bodies. As an example, Fig. 59a shows a configuration with two constraints (one DoF) whose instant center of rotation (O_m) is defined by the two dashed lines, further, the *exact constraint* of a rigid body in plane requires the presence of three constraints such as Fig. 59b.

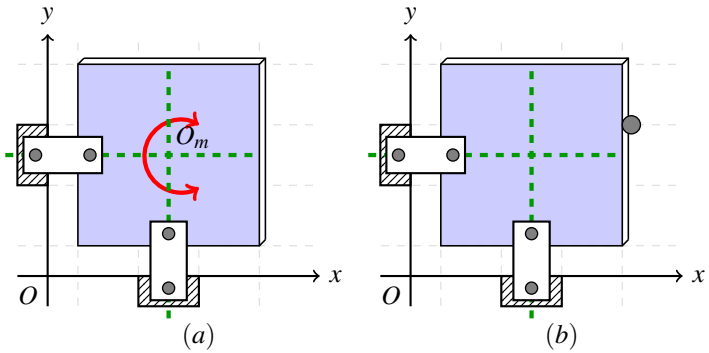

Figure 59: Two and three constraints of a rigid body in a plan.